DEFORMATION ET RUPTURE DES ALLIAGES CFC A BASSE EFE

IMPORTANCE DU MACLAGE MECANIQUE

A.Pineau

Centre des Matériaux - Mines ParisTech

andre.pineau@ensmp.fr

DEFORMATION ET RUPTURE DES ALLIAGES CFC A BASSE EFE

IMPORTANCE DU MACLAGE MECANIQUE

A.Pineau

Centre des Matériaux - Mines ParisTech

andre.pineau@ensmp.fr

STUDIES AT CDM DEVOTED TO TWINNING IN FCC MATERIALS

(To my knowledge)

- ≃ 1970 : A. Guimier & J.-L. Strudel – WASPALOY
- ≃ 1970-1980 : F. Lecroisey – L. Rémy – F. Abrassart – K. Sipos - G. Chalant – D. Fournier – A.Pineau

  Stainless Steels – Fe-Mn alloys – Co-Ni alloys – Inco 718
- ≃ 1970-1990 : J.-L. Strudel : Ni-base Superalloys
- ≃ 2008 : S. Nanga, Stainless Steels
- ≃ 2007-2010 : J. Lorthios, A.-F. Gourgues, J. Besson – TWIP Steels
- ≃ 2010 : S. Forest et al.

C.Efstathiou, H. Sehitoglu, Acta Mater., vol.58, 2010, pp. 1479-1488

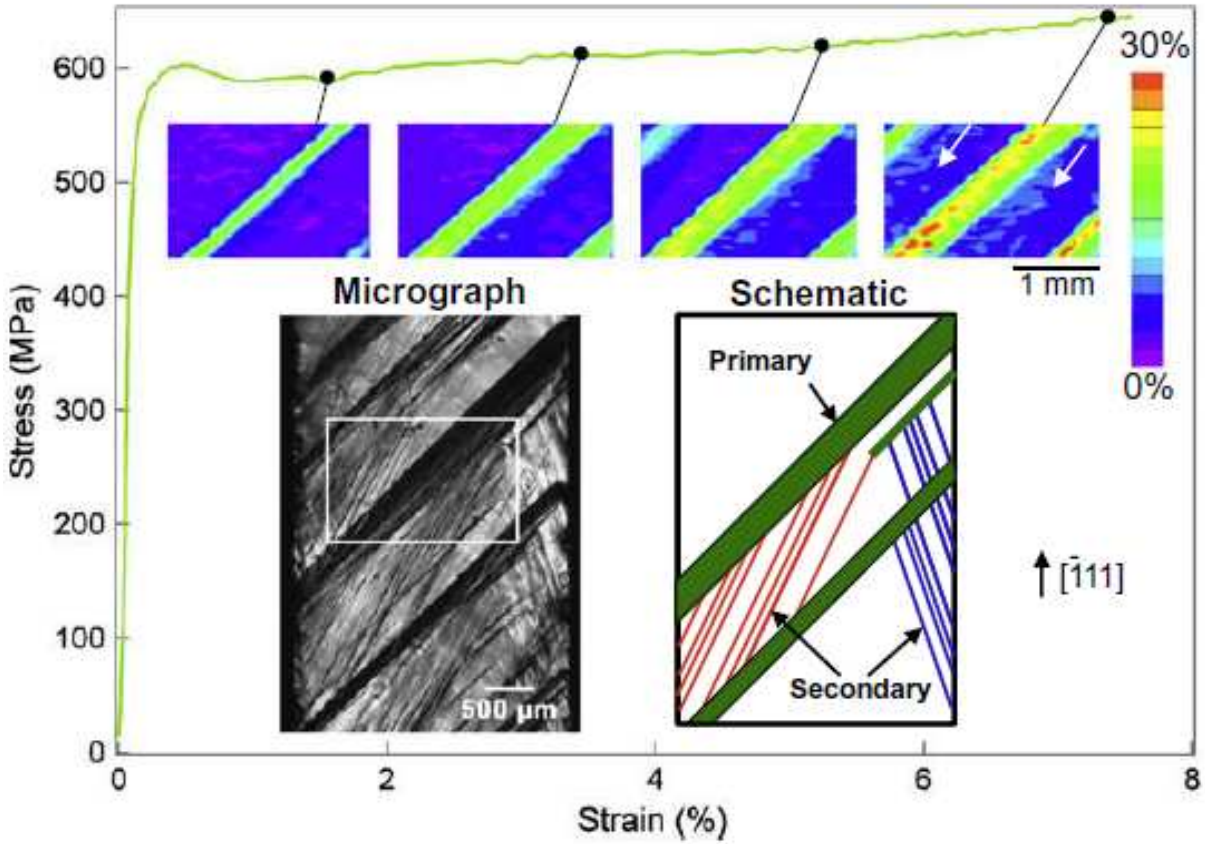

Hadfield Steel

Single Crystal

Fig. 4. The nominal stress–strain response, and the axial strain fields calculated from DIC at selected points along the curve. A post-deformation optical micrograph of the specimen surface with a white box indicates where the DIC strain fields are reported. Three twin-systems are identified, and for the purposes of clarity they are represented in the schematic as primary and secondary.

C.Efstathiou, H. Sehitoglu, Acta Mater., vol.58, 2010, pp. 1479-1488

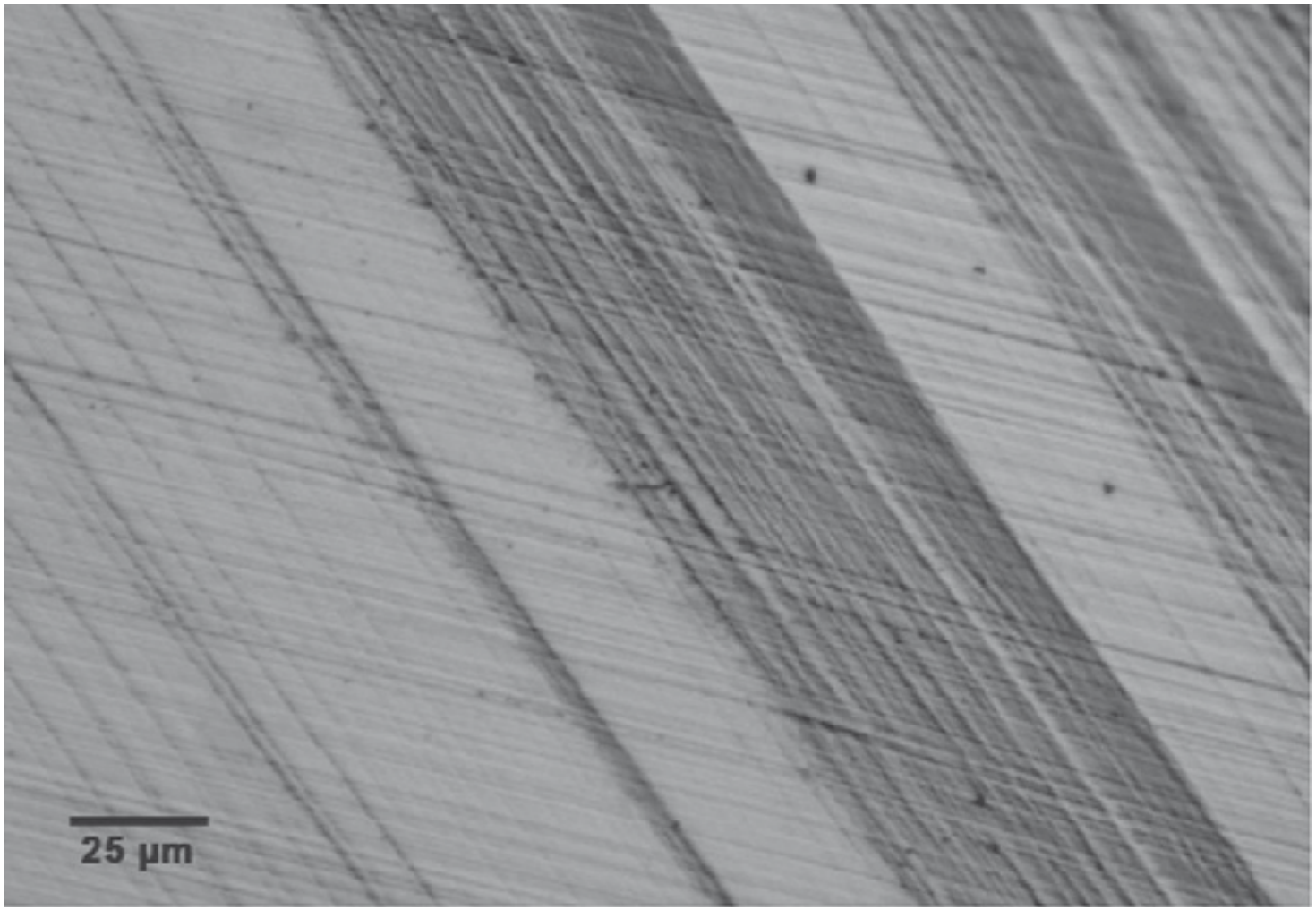

Hadfield Steel

Single Crystal

Fig. 1. An optical micrograph showing that twin-bands are composed of alternating layers of fine twin lamellae (black) and matrix material (white). Note that the inclination of the twins with respect to the tensile loading axis (vertical) is approximately 54°, which indicates they are from the primary twin system.

Fe-18Cr-18Mn-0.03C-0.6N

77K – ϵ = 9.2 %

P. Mullner, Acta metall. mater. ,vol.42,1994,pp.2211-2217

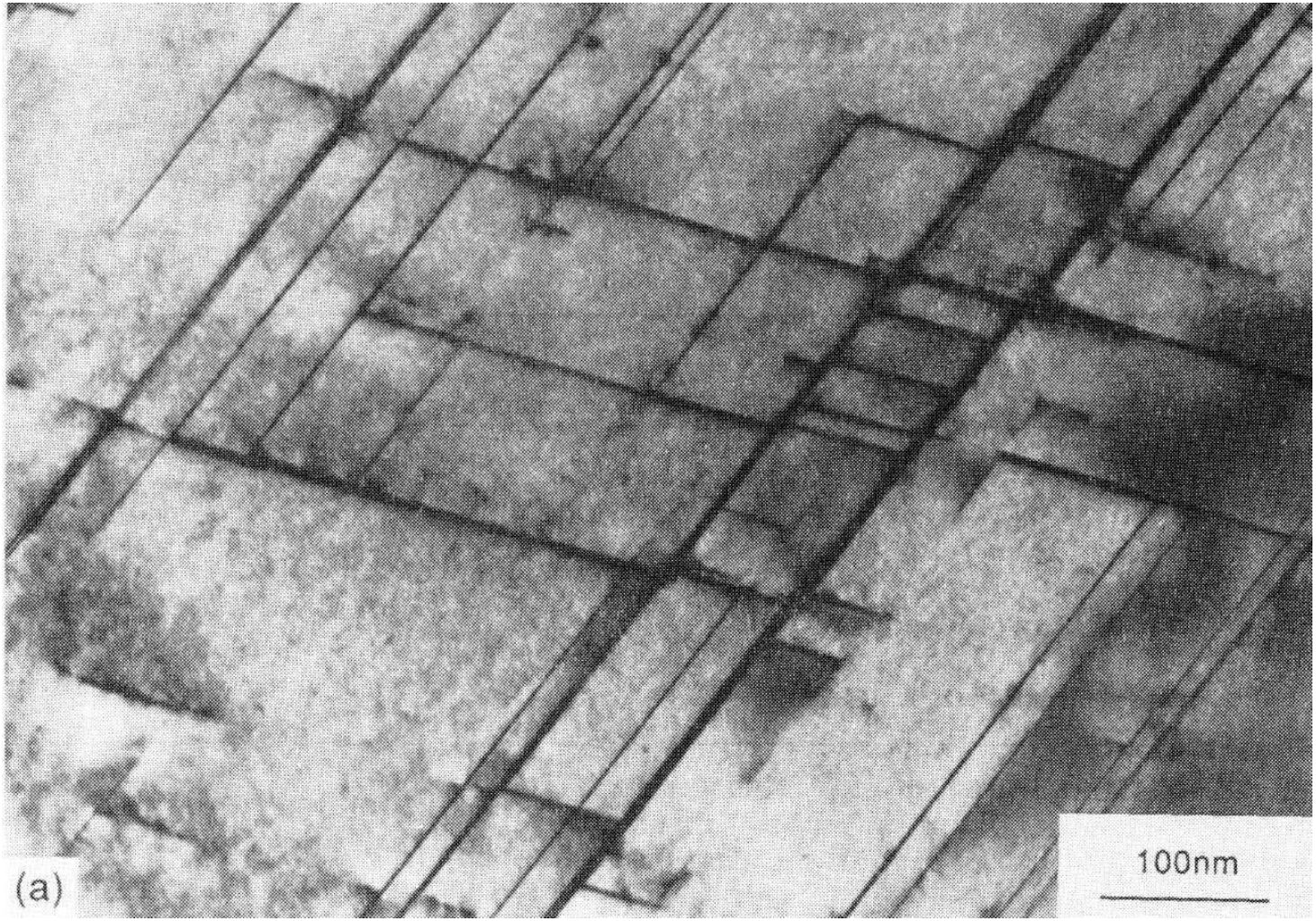

Fe-16Cr-17Ni-4Mn-3Mo-0.03C-0.26N

4.2K – ϵ = 32%

P. Mullner, Acta metall. mater. ,vol.42,1994,pp.2211-2217

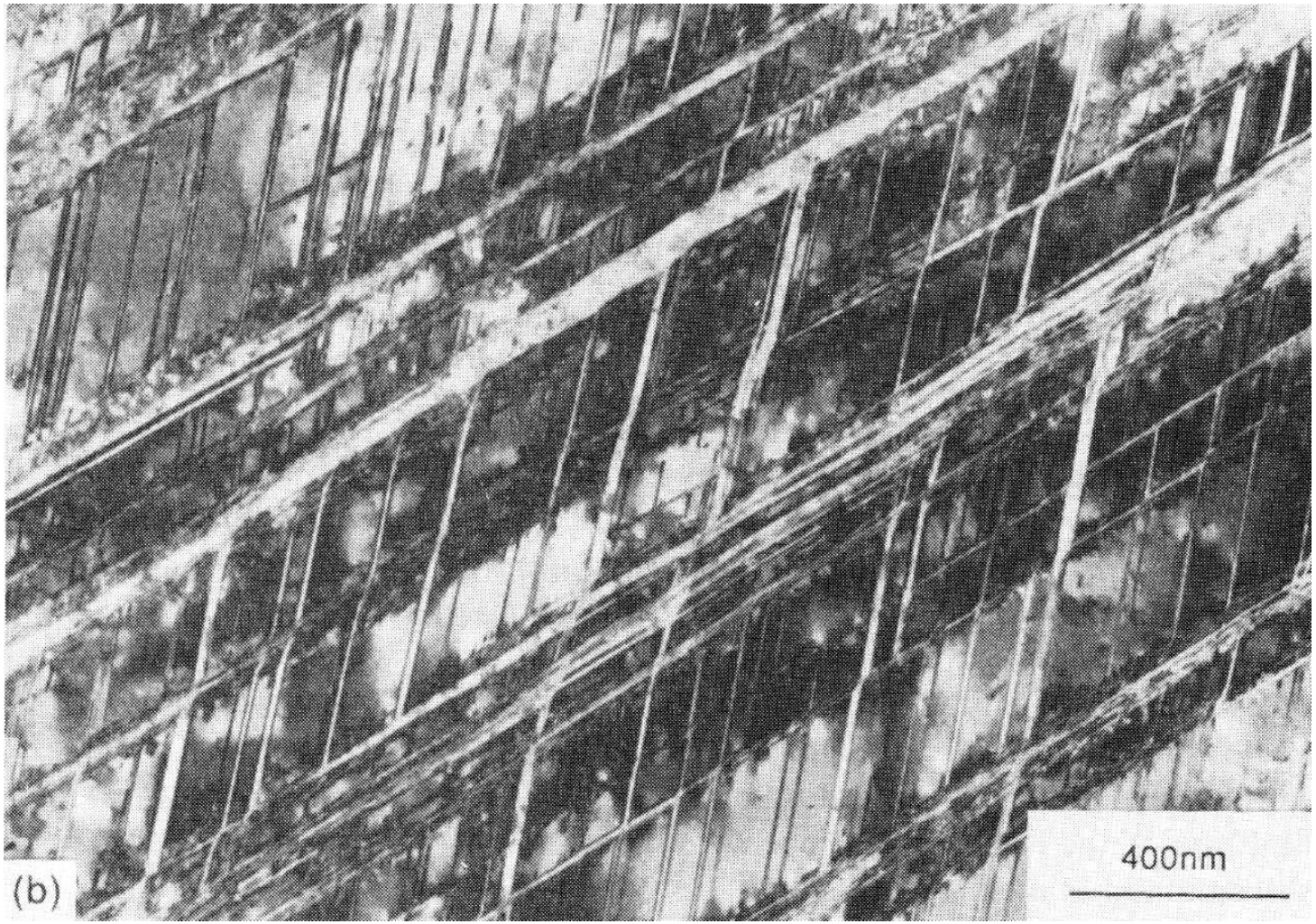

ACIER INOXYDABLE AUSTENITIQUE

L.Rémy, A.Pineau, Met. Trans ,1974, vol.5, p.963

Austenite

ε Martensite

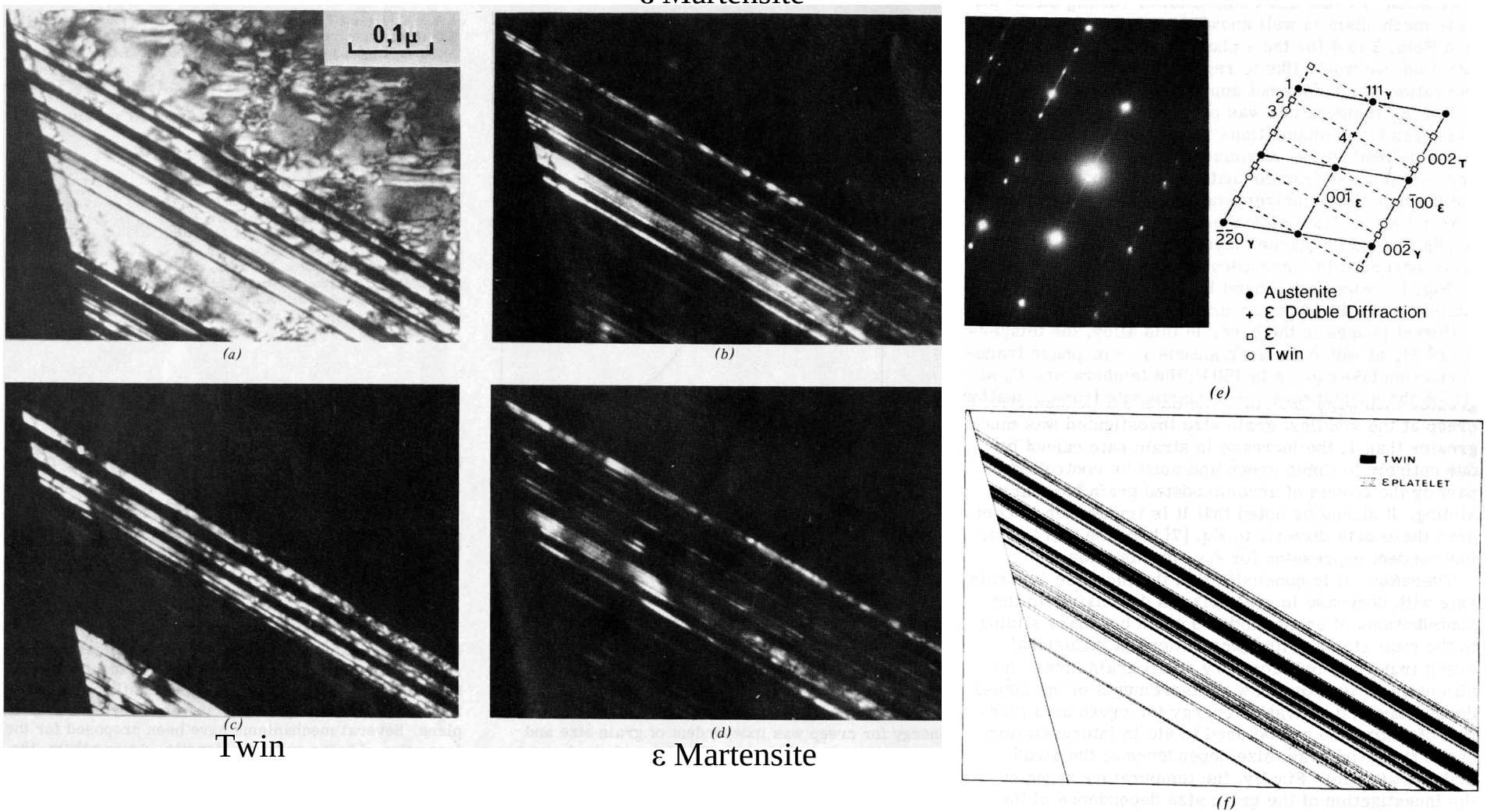

Twin

ε Martensite

TEM analysis of a band of twins and Є martensite : a), b), c), d) dark field images with diffraction spot 1,2,3 4; e) diffraction pattern (electron beam parallel to 1-10 austenite; f) schematic of the fine structure of the band

P. Mullner, Acta metall. mater. ,vol.42,1994,pp.2211-2217

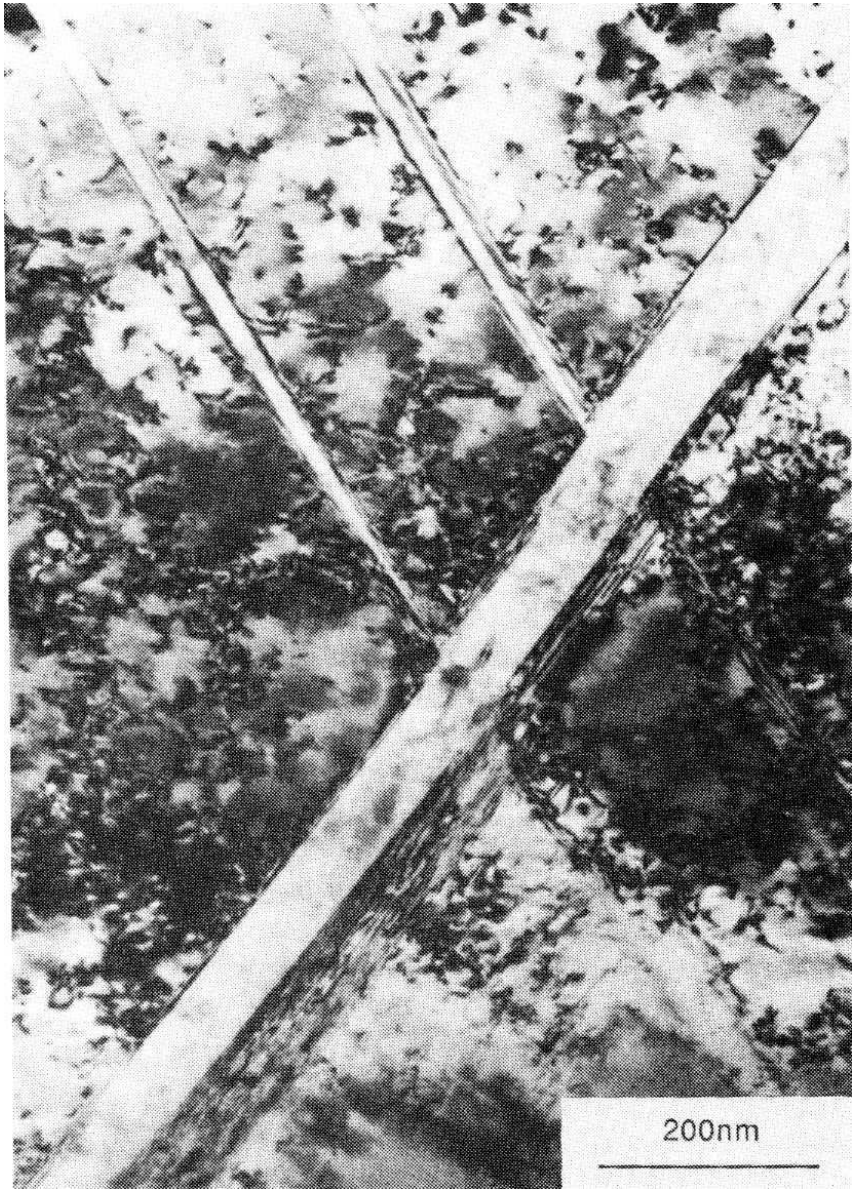

Fe-21Cr-13Ni-7Mn-3Mo-0.02C-0.39N

4.2K – ϵ = 8.2%

M.J. Marcinkowski, Trans AIME , vol.242, 1968, pp.1405-1412

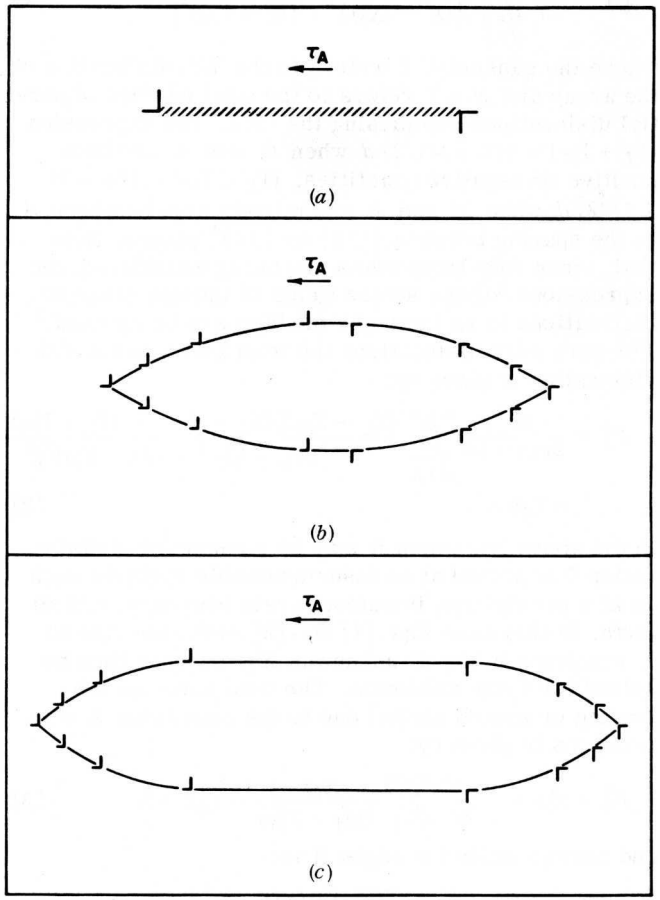

Fig. 1—(*a*) Stacking fault bounded by a pair of partial dislocations. (*b*) Array of partials arranged so as to form lenticular twin. (*c*) Array of partials arranged so as to form more extended twin.

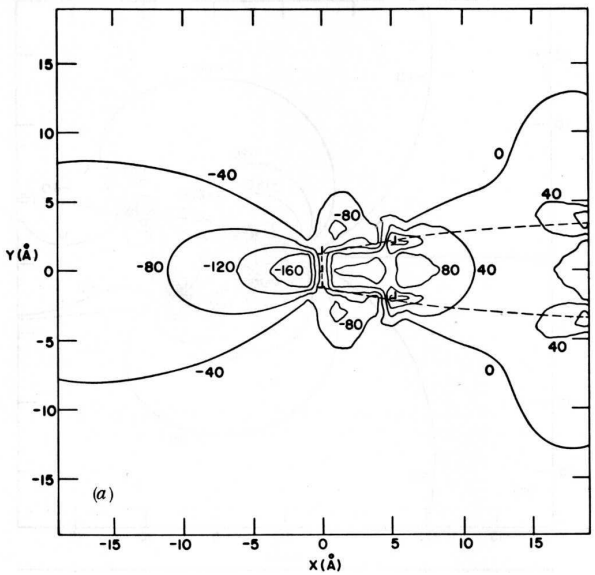

σ_{XY}

Unités

10^5 µb / (1-ν)

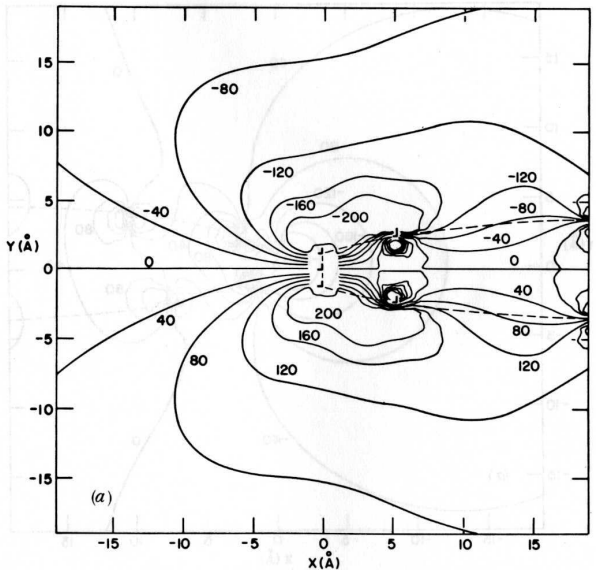

σ_{XX}

P. Mullner et al., Acta metall.mater.,vol.42,1994, pp.2211-2217

Fe-16Cr- 17Ni - 4Mn -3Mo - 0.03C- 0.26N

Tensile test

at 4.2 K

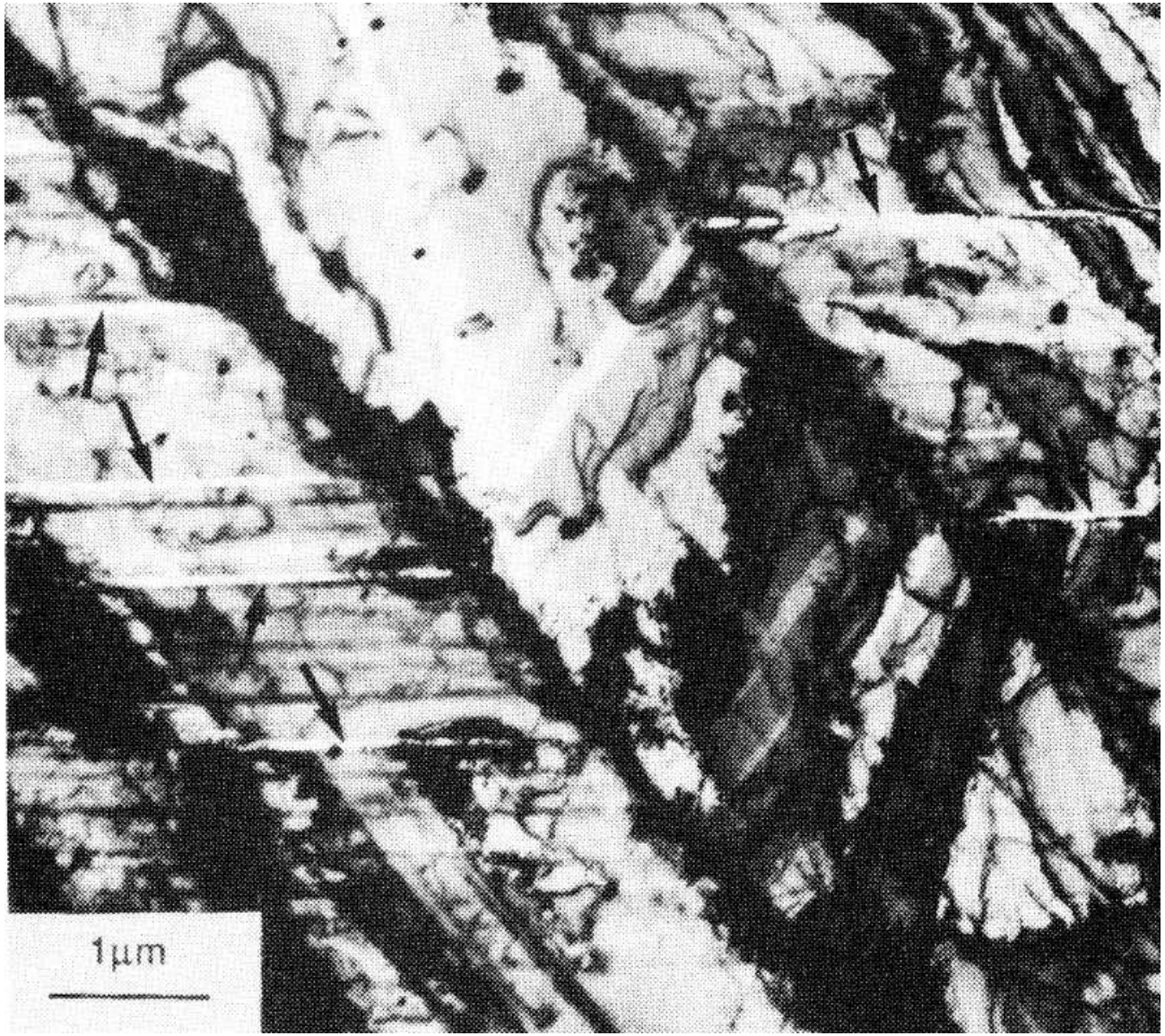

RESULTS

Effect of Temperature at low strain rate (3×10^{-4} s^{-1}) : 201 Steel

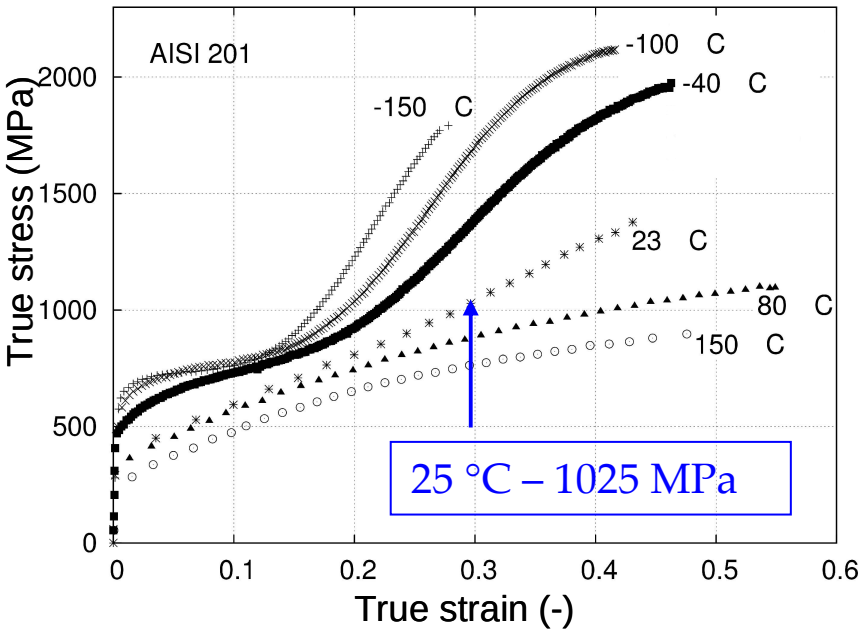

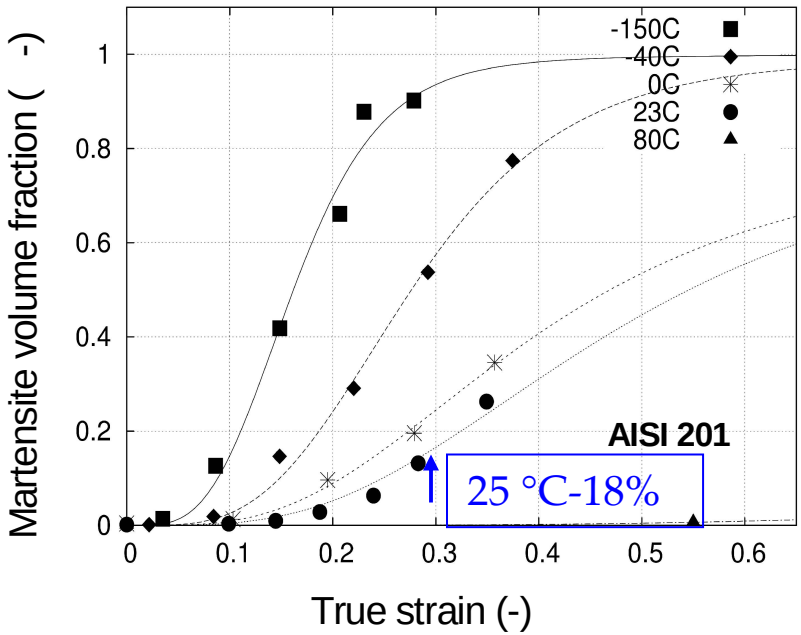

201 Steel is more stable than 301 LN Steel

20°C – $\dot{\epsilon}$ = 7 10^{-3} s^{-1} – Continuous loading

20°C – $\dot{\epsilon}$ = 7 10^{-5} s^{-1} – Continuous loading

20°C – $\dot{\epsilon}$ = 8 10^{-5} s^{-1} - 1st loading and unloading, then loading at 100°C

301 Steel

Ph. Pilvin, 2009

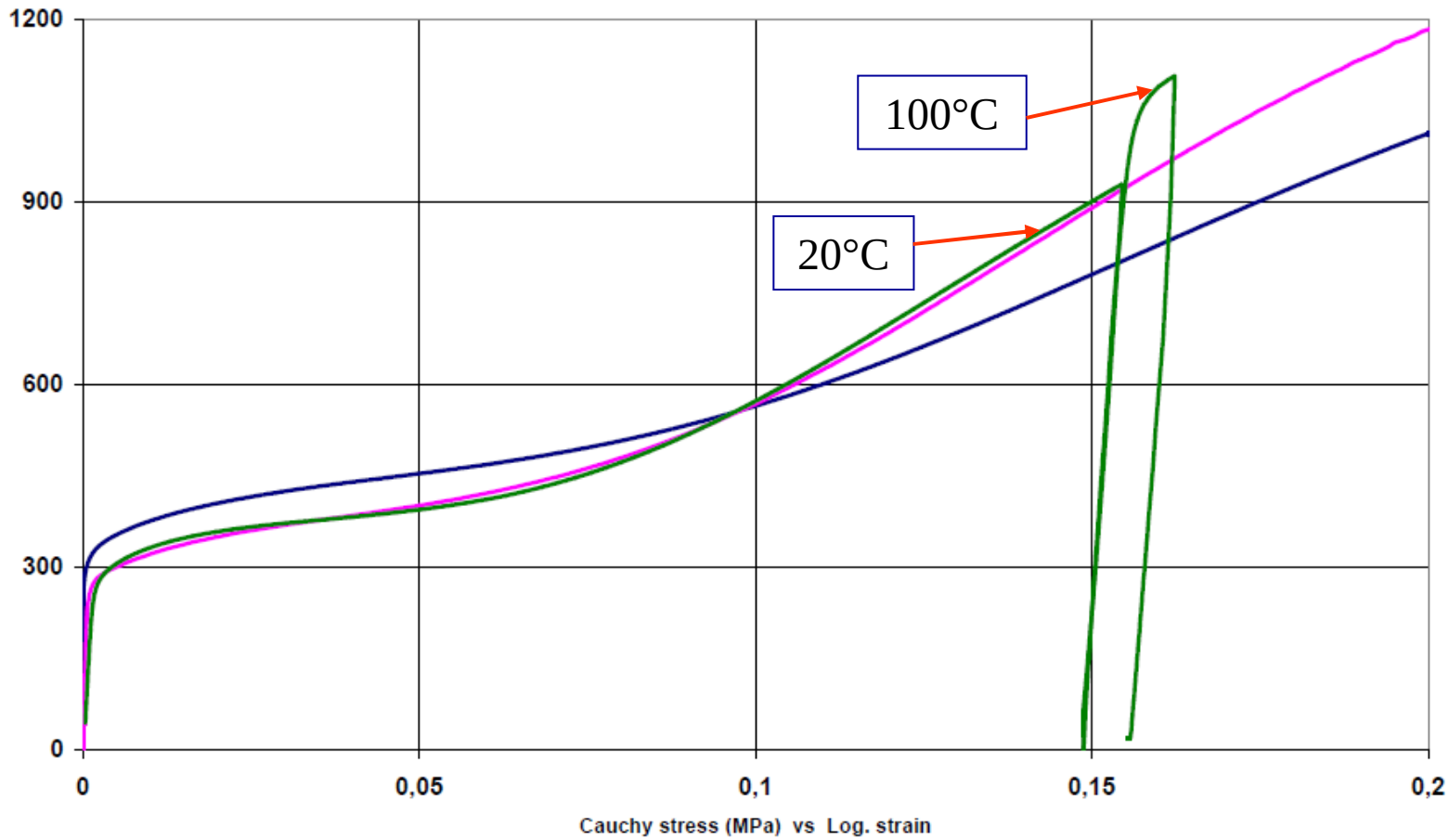

DEFORMATION TWINNING (in the absence of strain induced martensite) CAN PRODUCE EXTREMELY LARGE WORK- HARDENING RATES

L. Rémy, Acta Met.,vol.20, 1978, pp.443-451

Co-33Ni

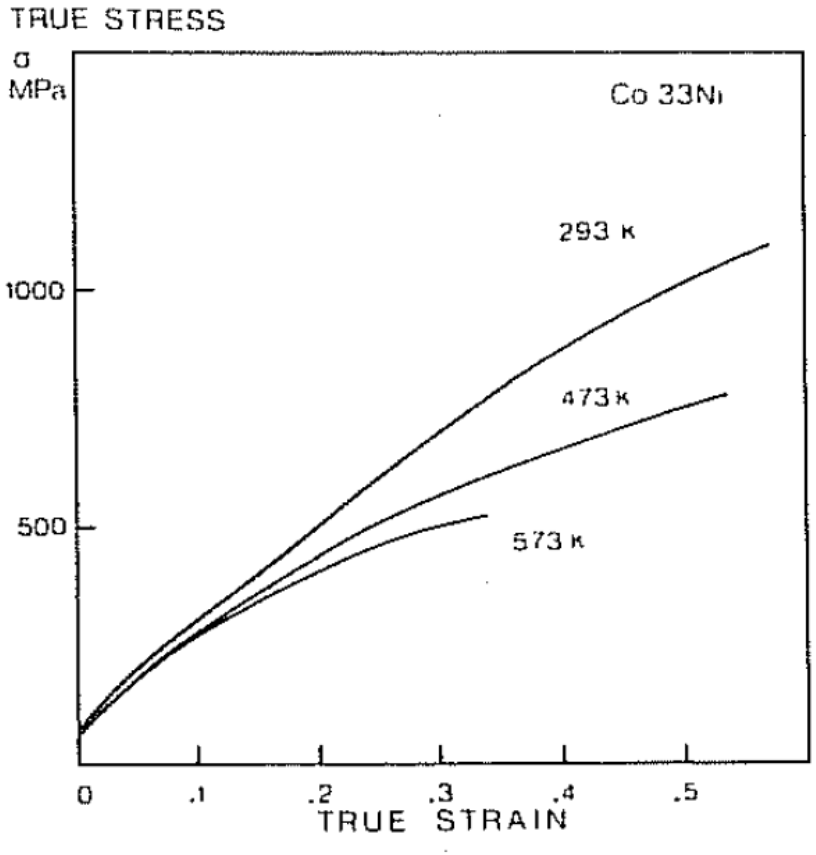

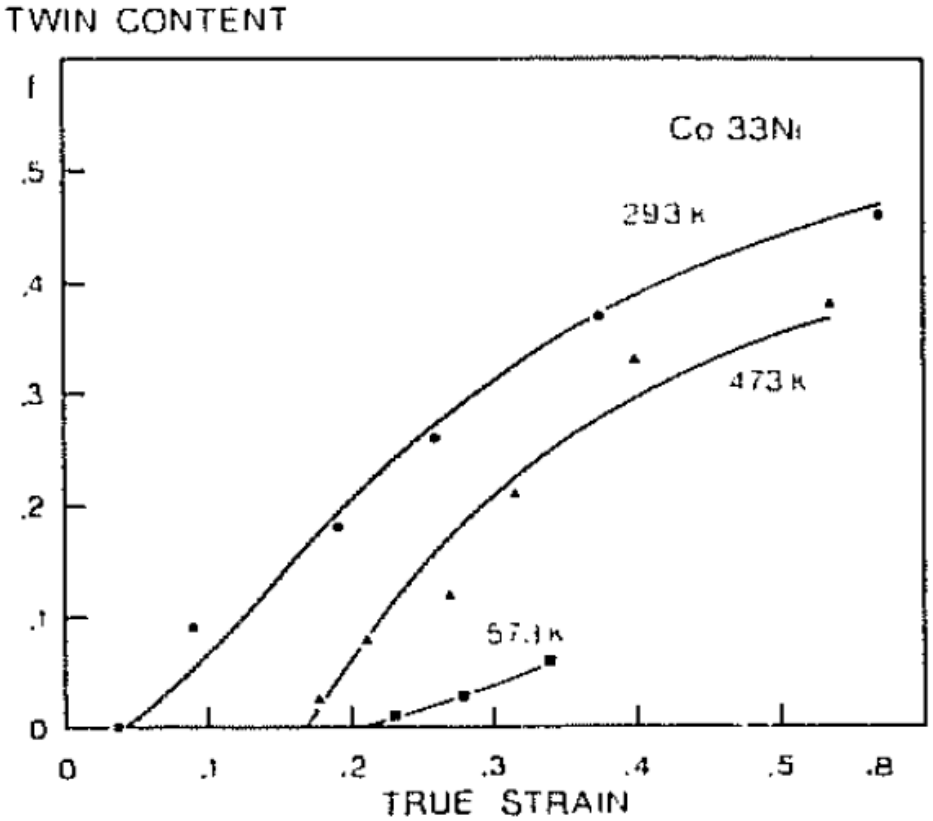

J.A. Venables, Deformation Twinning,, 1963

L. Rémy , Met.Trans., vol.12A, 1981,pp.387-408

L. Rémy et al;, Mat. Science & Eng.,vol.36,1978, pp.47-63

TWINNING STRESS ?

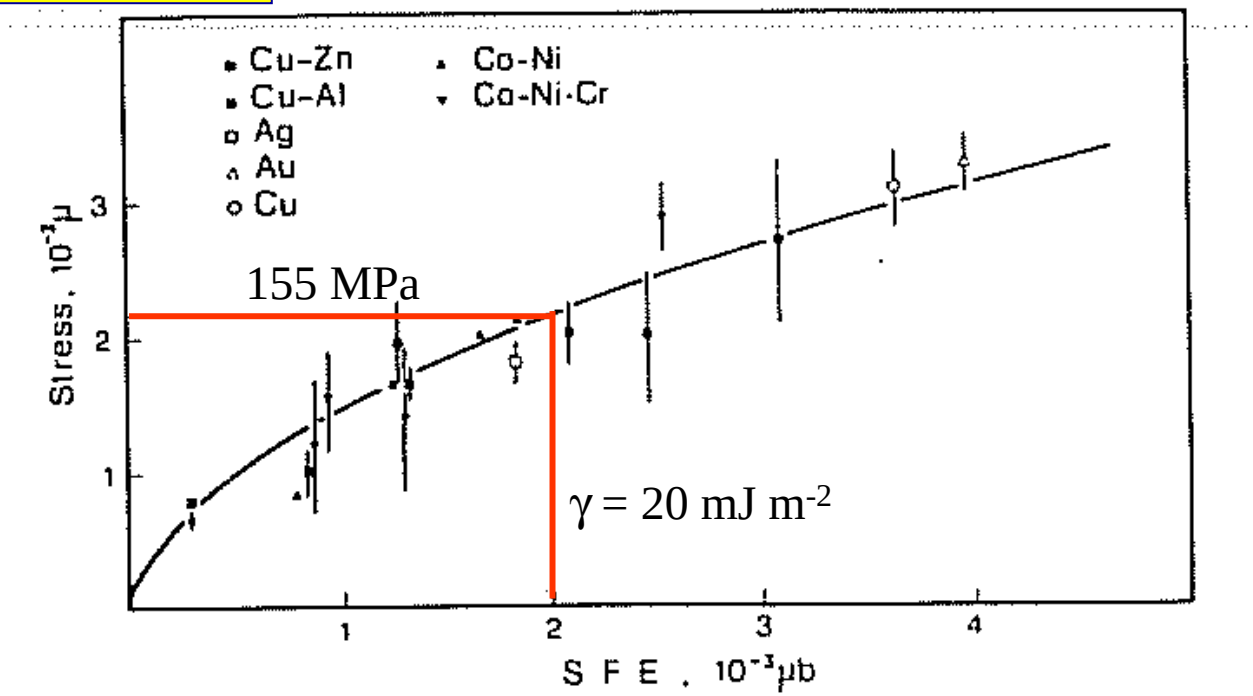

$$\frac{d\gamma}{dT} = \frac{8}{\sqrt{3}}\, a^2\, N\, \Delta S^{fcc \to hcp}$$

$$Fe - 19\,at\%Cr - 12\,at\%Ni \longrightarrow d\gamma / dT = 0.10\, mJ\, m^{-2}\, K^{-1}$$

$$Fe - 20\,at\%Mn - 4\,at\%Cr \longrightarrow d\gamma / dT = 0.06\, mJ\, m^{-2} K^{-1}$$

STRONG TEMPERATURE INFLUENCE in particular IN STAINLESS STEELS

DEFORMATION ET RUPTURE DES ALLIAGES CFC A BASSE EFE

IMPORTANCE DU MACLAGE MECANIQUE

A.Pineau

Centre des Matériaux - Mines ParisTech

andre.pineau@ensmp.fr

1. INTRODUCTION

2. INTERACTIONS ENTRE MACLES (See also J.W. Christian & S. Mahajan, *Deformation Twinning , Progress in Materials Science, vol.39, pp.1-157, 1995)*

3. MACLAGE (et Déformation planaire) ET RUPTURE (Intergranulaire)

- **3.1. Intersections entre macles mécaniques et macles de recuit**
- **3.2. Maclage et Rupture Intergranulaire**
  - **Fatigue – Fluage et Fatigue- Fluage**

4. REHEAT CRACKING DES ACIERS INOXYDABLES AUSTENITIQUES

- **4.1. Une expérience astucieuse**
- **4.2. Autres résultats sur divers aciers**

5. CONCLUSIONS

C.Efstathiou, H. Sehitoglu, Acta Mater., vol.58, 2010, pp. 1479-1488

Hadfield Steel

Single Crystal

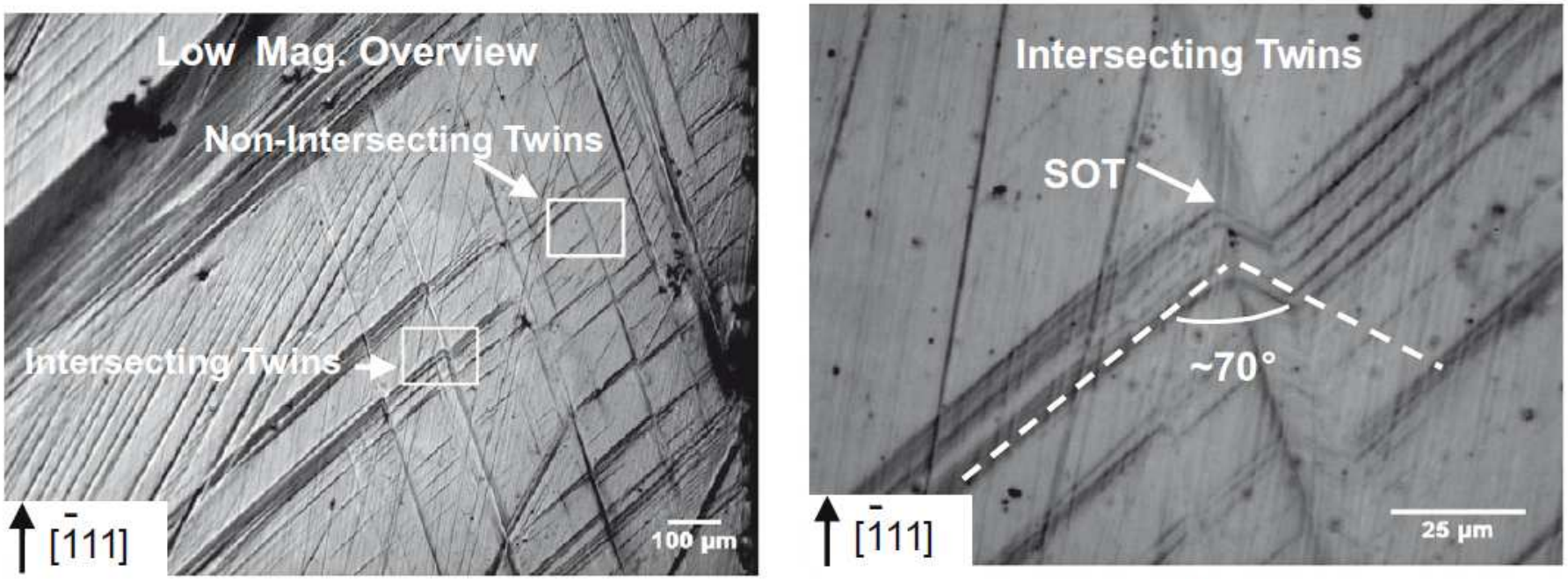

(a) 5x (b) 50x

Fig. 5. Optical micrographs showing the intersection of twin-bands after moderate applied deformation (less than 10% strain). (a) Low-magnification overview shows all three twin-systems (one primary and two secondary) have activated. Some regions show intersecting twins, whereas others show non-intersecting twins. (b) A high-magnification detail of a twin–twin intersection which has formed a second-order twin (SOT). (c) A high-magnification detail of a non-intersecting twin.

C.Efstathiou, H. Sehitoglu, Acta Mater., vol.58, 2010, pp. 1479-1488

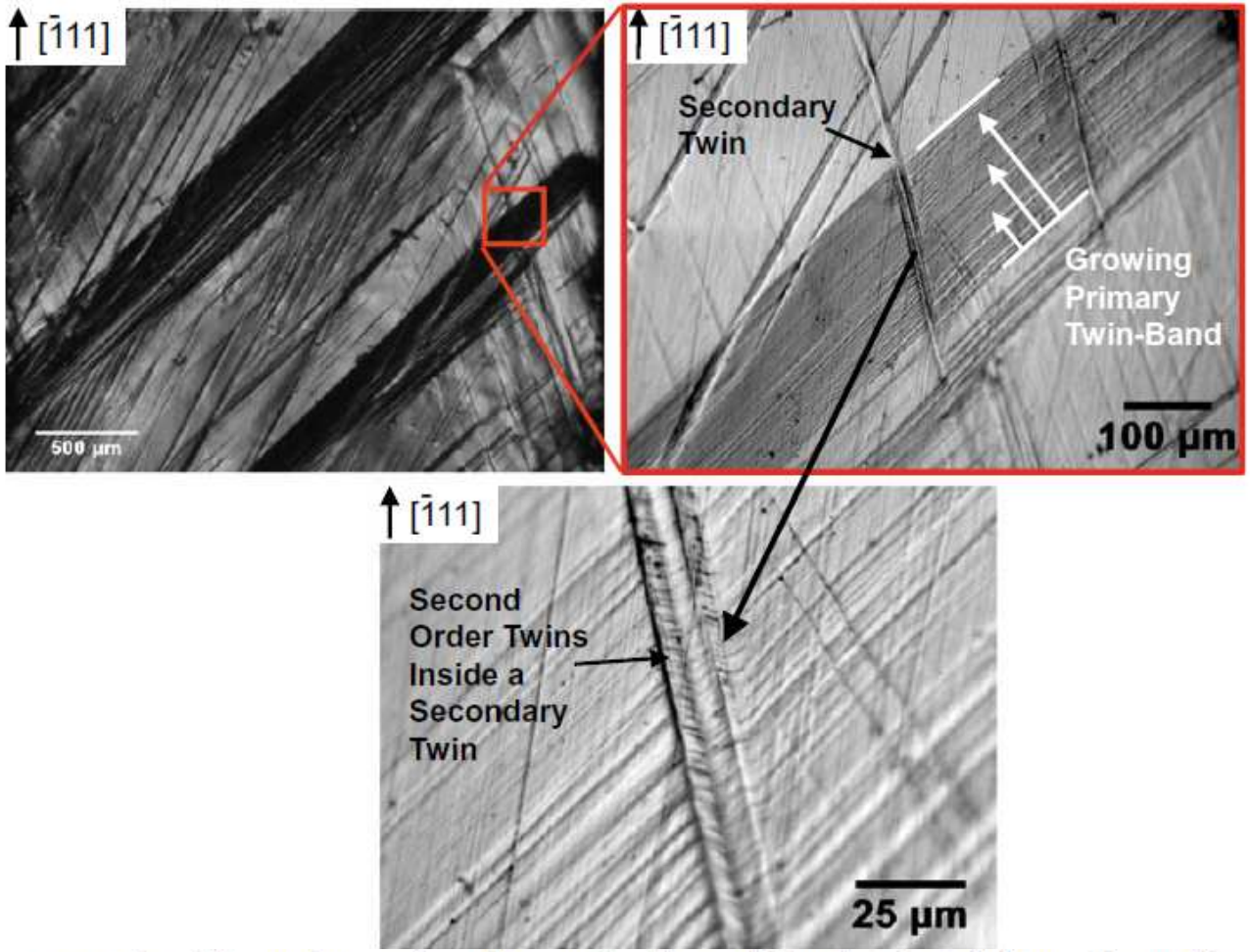

Hadfield Steel

Single Crystal

Fig. 7. Shows an overview of the specimen surface with a small red box outlining the twin–twin intersection, and increasingly higher-magnification images showing the second-order twins.

K.Rajan, J.Materials Science Letters, 1982, vol.1, pp.482-484

Co-Cr-Mo ALLOY

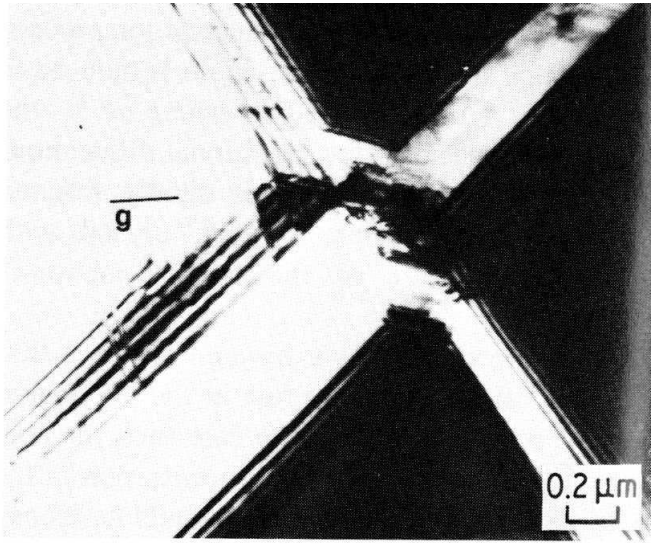

Figure 1 Twin-twin intersection; $\vec{z} = (1\bar{1}0)$, $\vec{g} = (111)$.

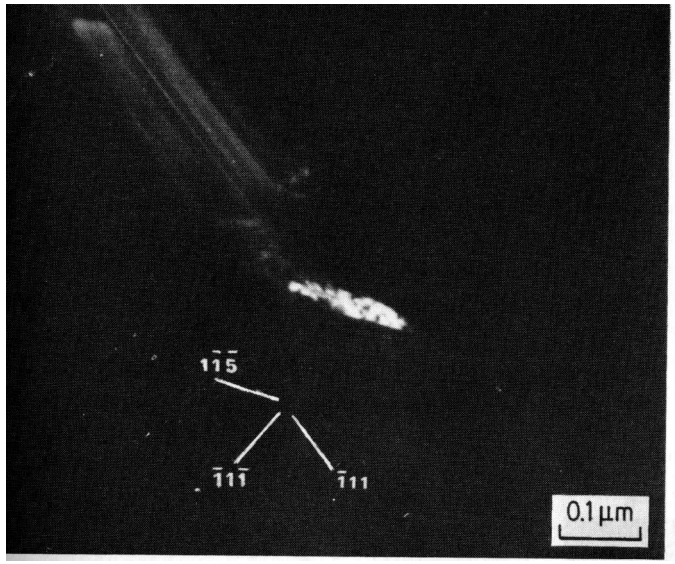

Figure 3 Dark-field image of secondary twins, using the $\{111\}$ secondary twin reflection. The traces of the $(\bar{1}1\bar{1})$, $(\bar{1}11)$ and $(1\bar{1}\bar{5})$ planes on the (110) plane are indicated; $\vec{z} = (110)$.

L. Rémy , Met. Trans., vol.12A , 1981, pp.387-408, *A.Coujou et al., Acta metall. mater.,vol.40, 1992,pp.337-344*

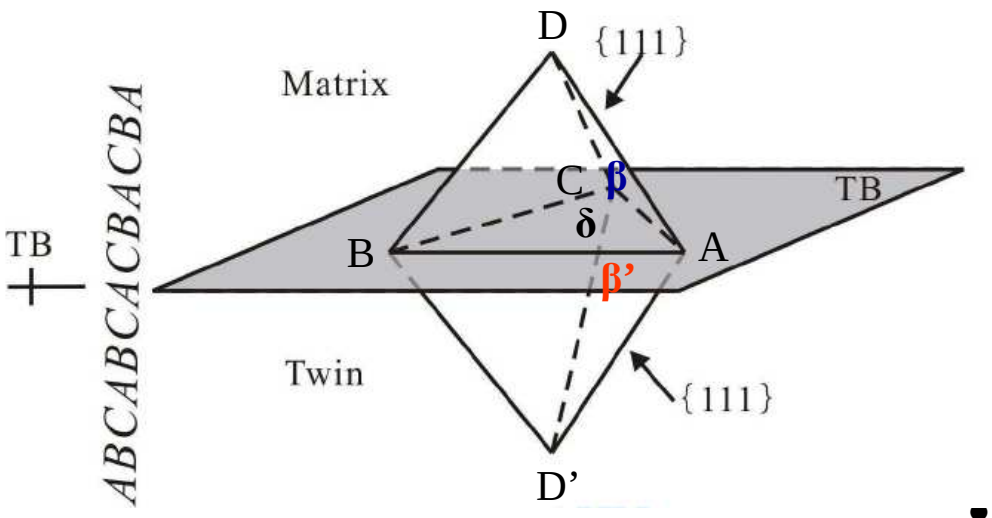

DISLOCATIONS PARFAITES

Les 2 partielles doivent se recombiner

- $AB \rightarrow Cross\ slip$
- $DC_\beta \rightarrow CD'_{\beta'} + 2\delta C_\delta \ (Twinning)$

$$\frac{1}{2}[110] \rightarrow \frac{1}{2}[110]_T + 2\times\frac{1}{6}\left[11\bar{2}\right] \quad (133\%)$$

- $DC_\beta \rightarrow AD'_{\beta'} + B\delta_\delta \ (Chgt\ épaisseur\ macle)$

$$\frac{1}{2}[110] \rightarrow \frac{1}{2}[101]_T + \frac{1}{6}\left[\bar{2}\bar{1}\bar{1}\right] \quad (33\%)$$

DISLOCATIONS PARTIELLES

- $3D\beta_\beta \rightarrow AD'_{\beta'} + CD'_{\beta'} + 2B\delta_\delta$

$$3\times\frac{1}{6}[211] \rightarrow \frac{1}{2}[101]_T + \frac{1}{2}[110]_T + 2\times\frac{1}{6}\left[21\bar{1}\right]$$

- $3\times D\beta_\beta \rightarrow CD'_{\beta'} + DC_\beta + B\delta_\delta$

$$3\times\frac{1}{6}[211] \rightarrow \frac{1}{2}[110]_T + \frac{1}{2}[110] + \frac{1}{6}\left[2\bar{1}\bar{1}\right]$$

$(Coujou, 1992)\ (Changement\ épaisseur\ macles)$

L.Rémy , Met Trans , vol.12A, 1981, pp.388-408

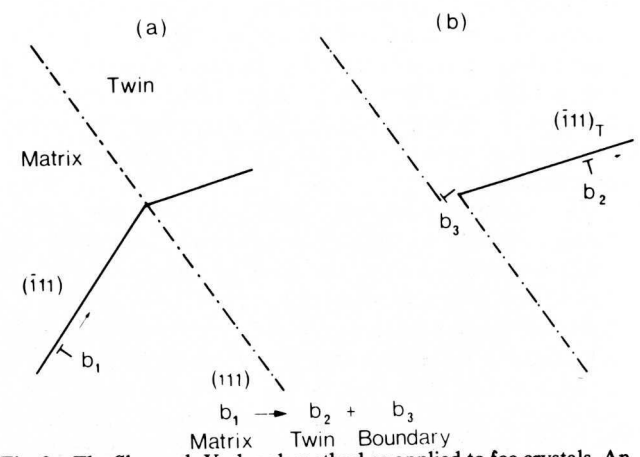

Fig. 3—The Sleeswyk-Verbraak method as applied to fcc crystals. An incident matrix dislocation with Burgers vector $\mathbf{b}_1$ impinging the twin boundary (*a*) has to dissociate into a dislocation in the boundary $\mathbf{b}_3$ and a twin dislocation $\mathbf{b}_2$ which slips on the mirror plane of the incident slip plane (*b*).

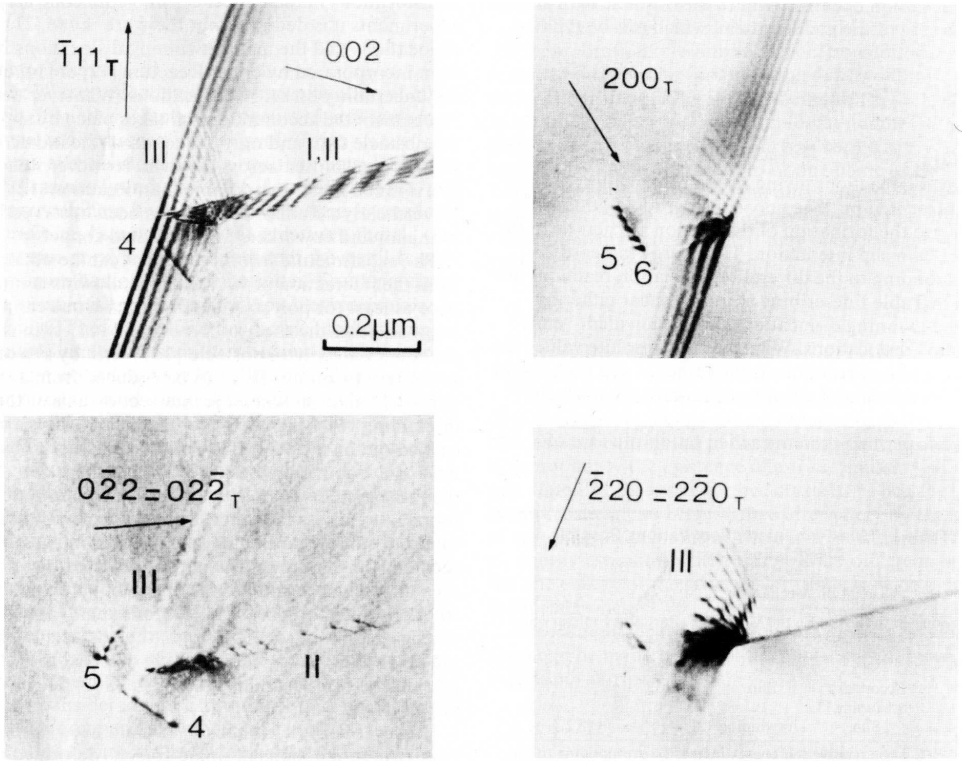

Fig. 7—Interaction of a thin deformation twin with an annealing twin boundary in cobalt-base alloy (taken from Ref. 10). Incident set I twinning dislocations are incorporated into the annealing twin by a dissociation into three product dislocations: set II dislocations reemitted in the mechanical twin, set III dislocations left at the boundary and slip dislocations in the annealing twin one of which is visible and dissociated into partials 5 and 6.

Cu- 5.5 at% Si *A.Coujou, Acta Met., vol.40,1992, pp.337-344*

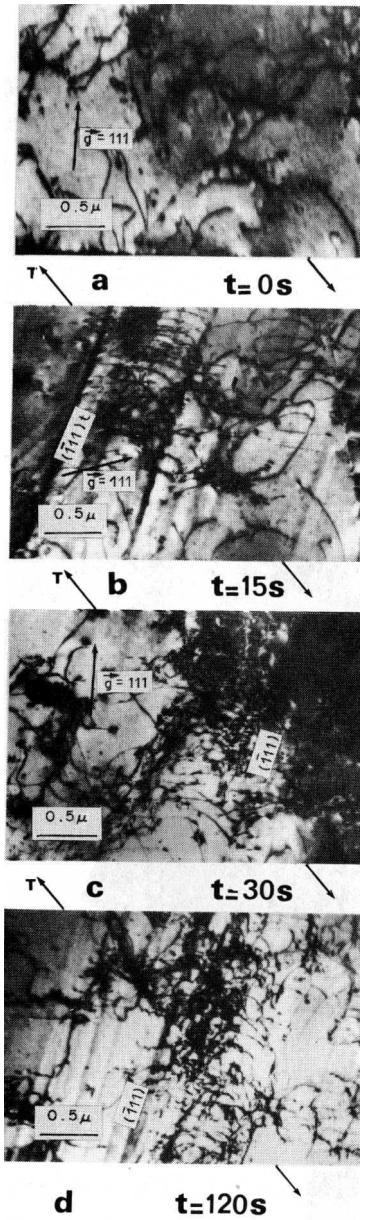

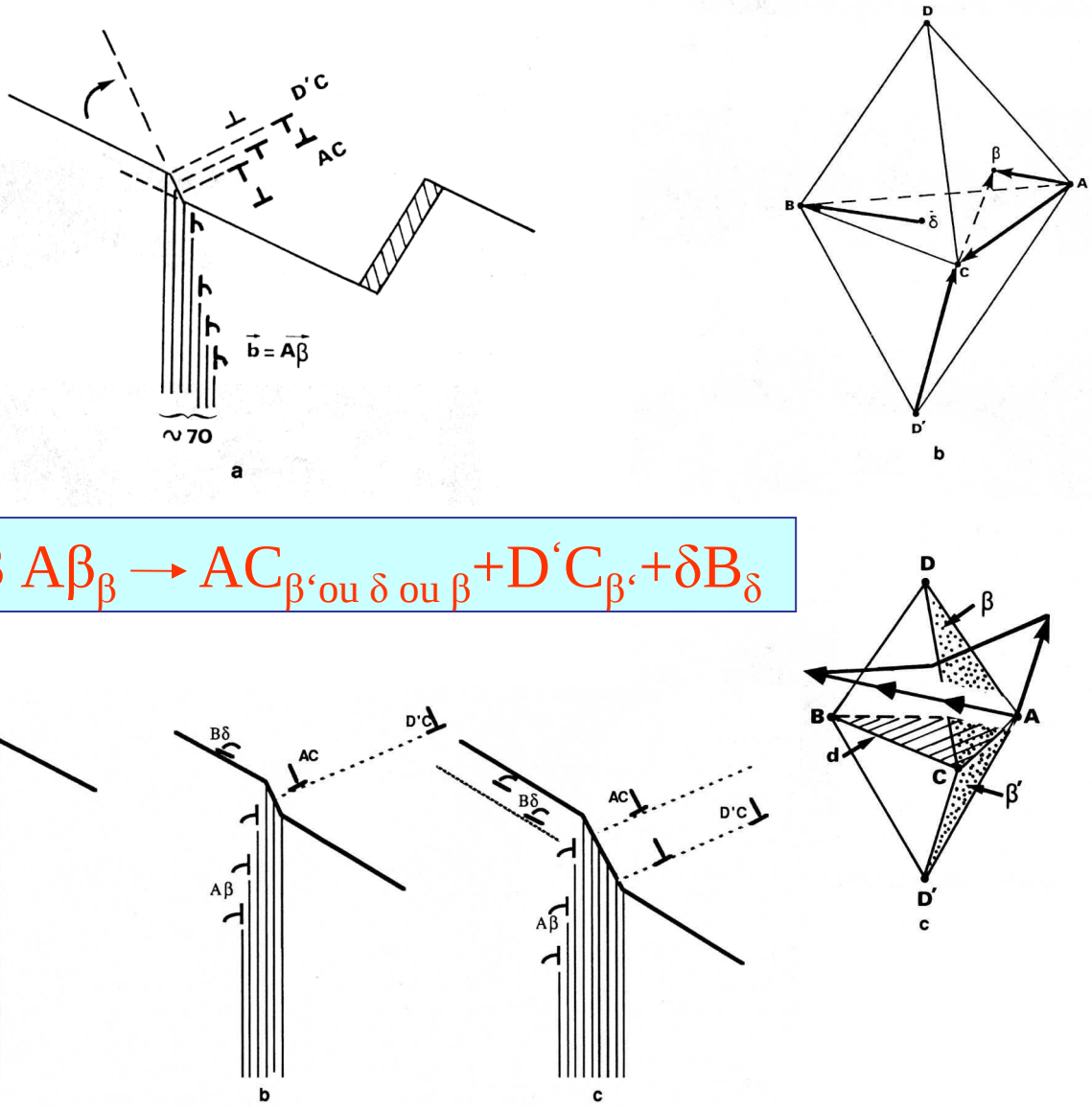

$$3\ A\beta_{\beta} \rightarrow AC_{\beta' \text{ou } \delta \text{ ou } \beta} + D'C_{\beta'} + \delta B_{\delta}$$

Fig. 8. Trois étapes de la transmission du cisaillement au joint de macle. (a) Arrivée de la tête de macle. (b) Réaction avec le premier triplet de partielles. (c) Intégration du second triplet de partielles.

Cu - 6.5 at.% Si

A. Coujou, Phil. Mag. Letters. 1987, vol.56 ,pp.13-21

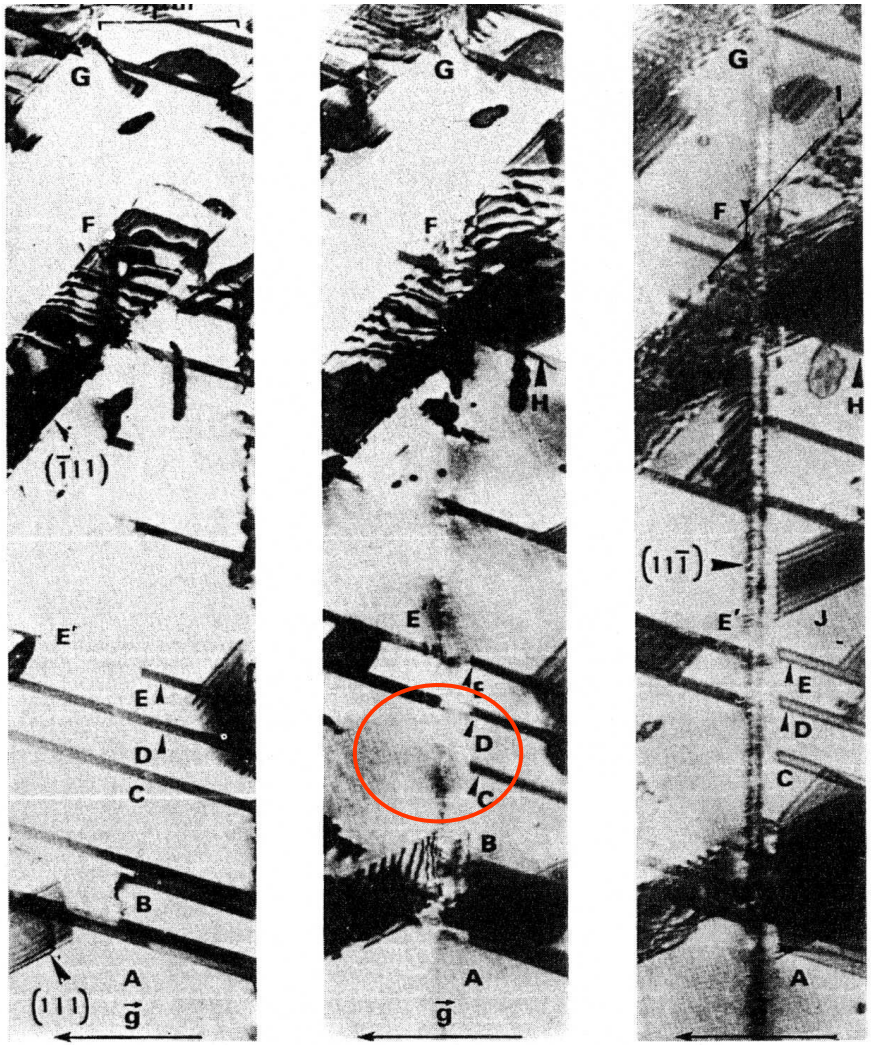

(*a*) (*b*) (*c*)

Ces trois clichés présentent, dans la même condition de contraste $\mathbf{g}=|\bar{1}11|$, trois états de déformation. La MM qui naît dans la région S se propage de bas en haut sur le cliché. Elle cisaille les défauts A, B, C, D, E ainsi qu'une MM secondaire en F.

Les fines macles ou défauts plans peuvent disparaître.

Les joints de macles ne sont pas infranchissables

Cu - 6.5 at.% Si

A. Coujou, Phil. Mag. Letters. 1987, vol.56 ,pp.13-21

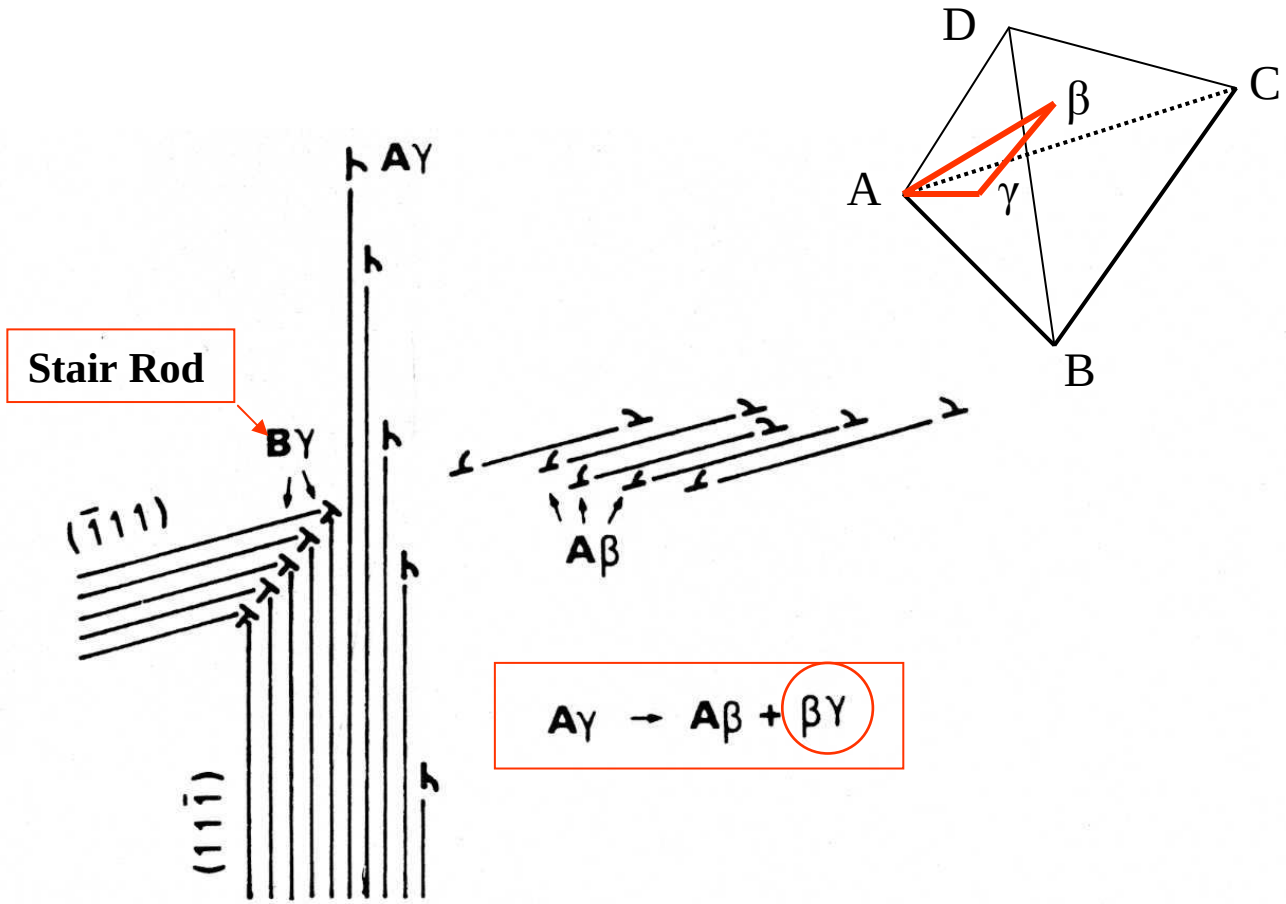

Schéma représentant l'intersection de deux MM telle qu'on peut l'observer dans la région F de la fig. 1. A la fin de l'intersection, les partielles de vecteur de Burgers $\boldsymbol{\beta}$A émises dans le plan ($\bar{1}11$) de la MM obstacle selon la réaction $\mathbf{A}\gamma \rightarrow \mathrm{A}\boldsymbol{\beta} + \beta\gamma$, se recombinent avec les dislocations partielles du front de la MM incidente pour redonner des dislocations parfaites dissociées sur des plans superposés (en F, fig. 1 (*c*)).

DEFORMATION ET RUPTURE DES ALLIAGES CFC A BASSE EFE

IMPORTANCE DU MACLAGE MECANIQUE

A.Pineau

Centre des Matériaux - Mines ParisTech

andre.pineau@ensmp.fr

P. Mullner et al., Acta metall.mater.,vol.42,1994, pp.2211-2217

Fe-16Cr- 17Ni - 4Mn -3Mo - 0.03C- 0.26N

Tensile test

at 4.2 K

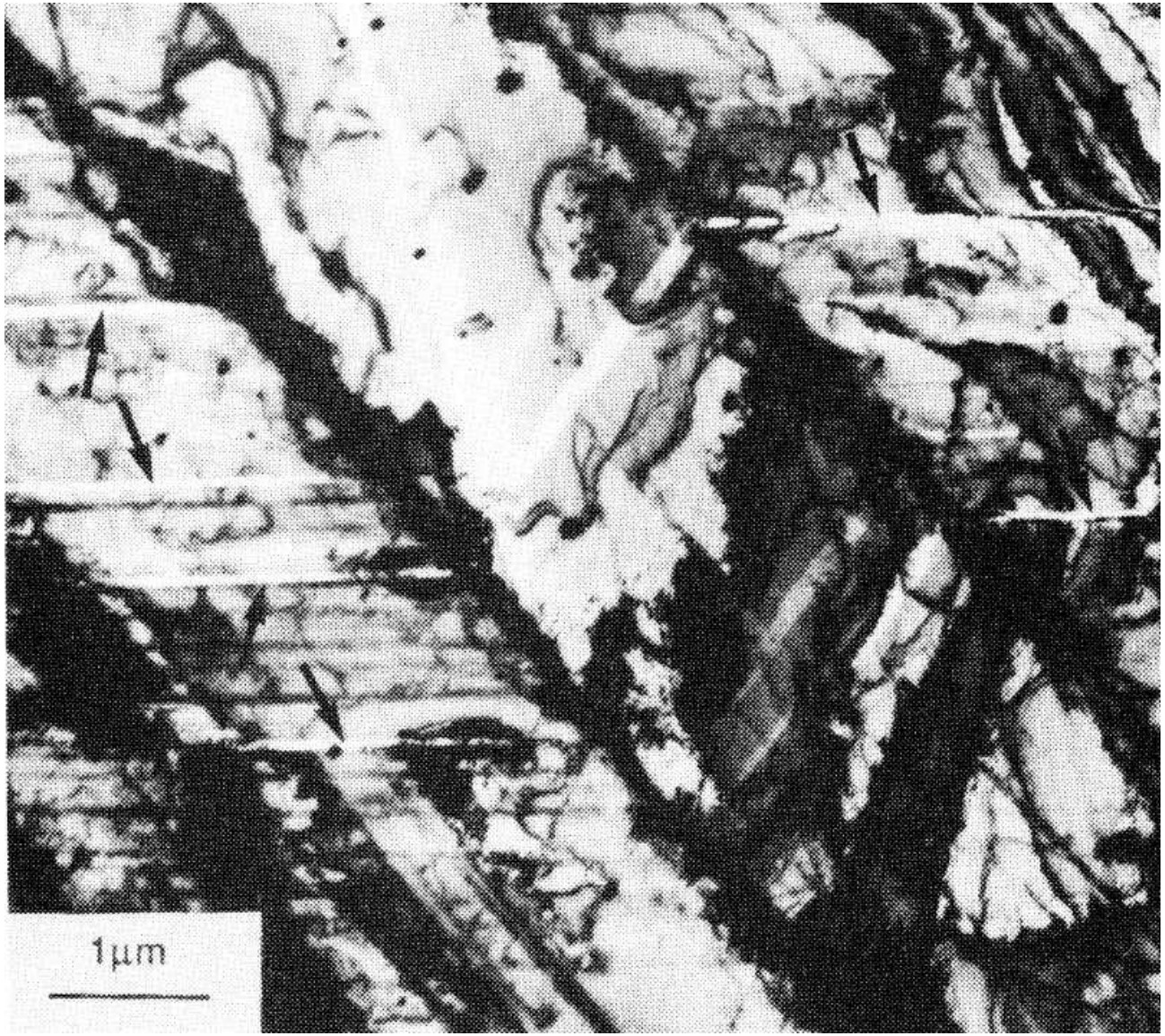

Hull, Acta Mat.,vol.8,1960, p.11

MONOCRISTAUX Fe-3Si

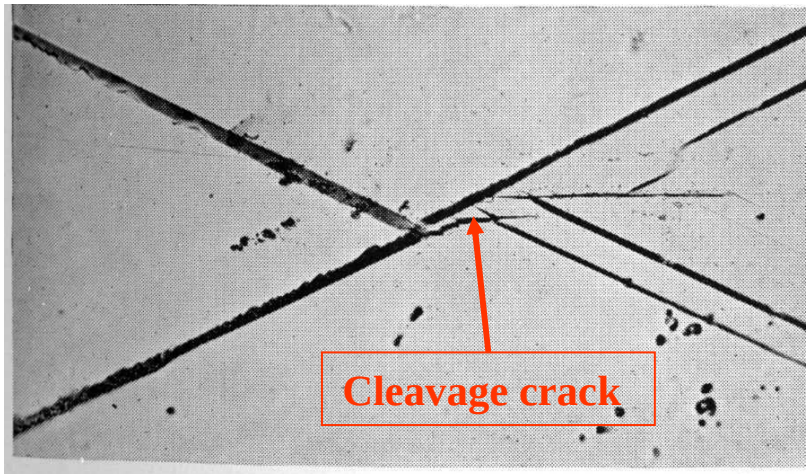

FIG. 11. An *A–D* type twin intersection producing a crack. ×140.

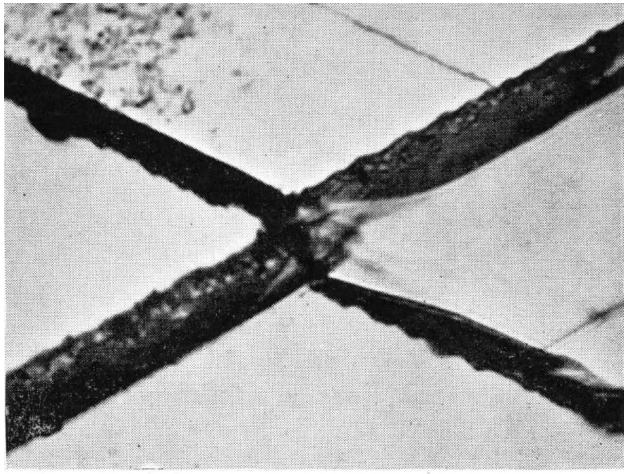

FIG. 13. An *A–D* type intersection that has not formed a crack. ×1000.

Z.F. Zhang et al., to be published in Phil. Mag.,2010

Cu-Zn & Cu-Al Alloys

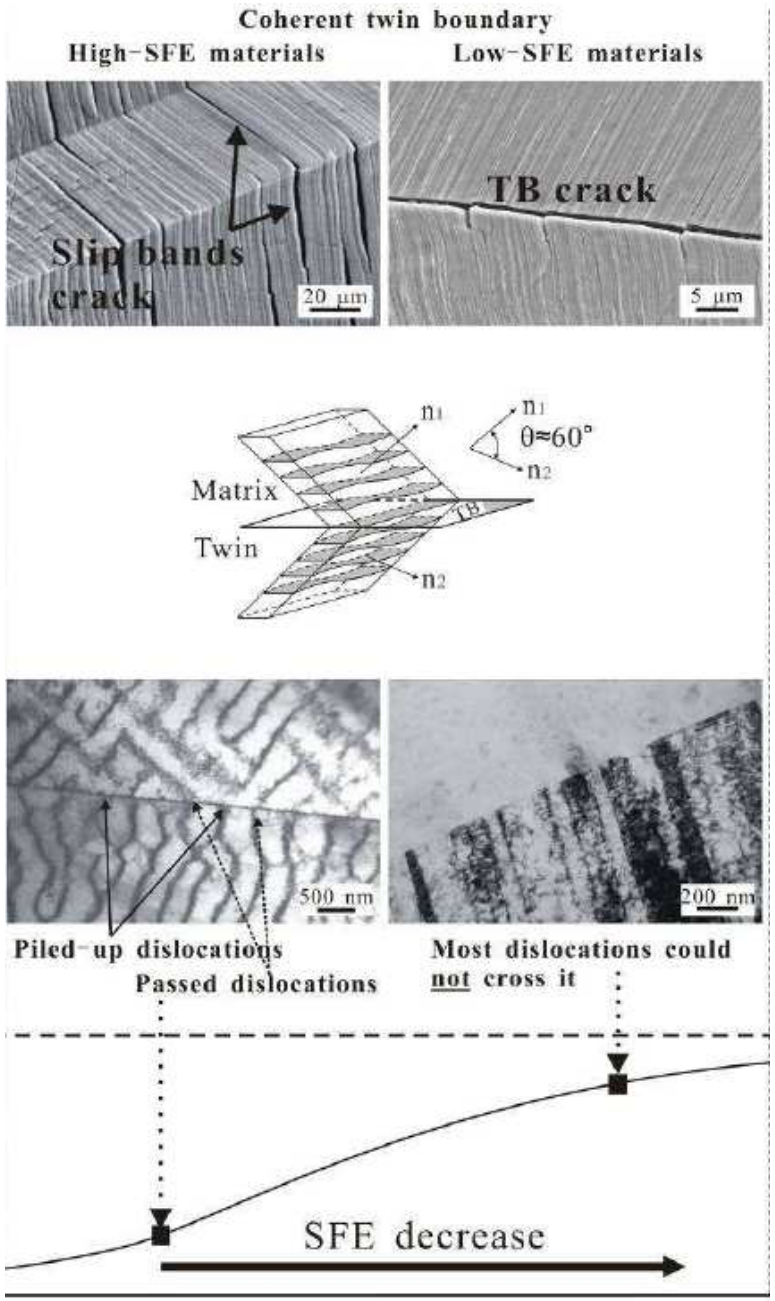

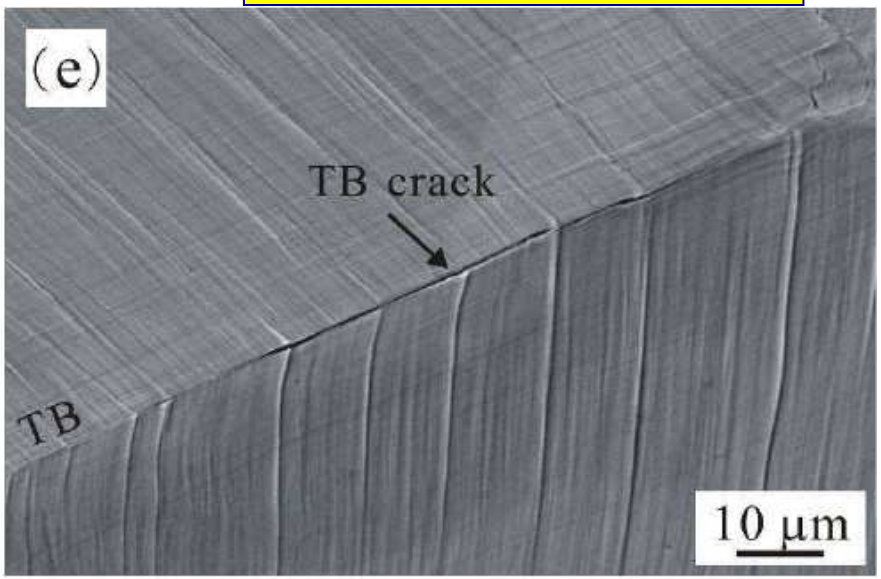

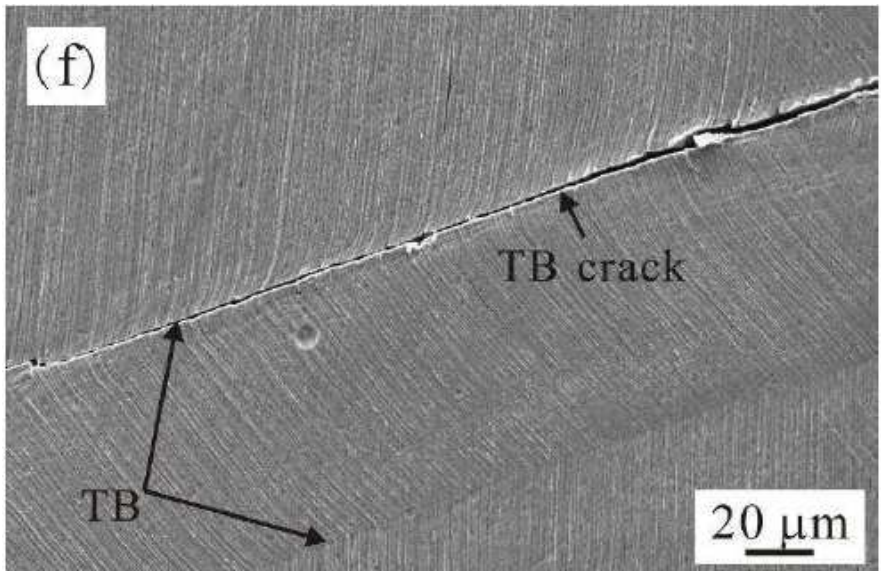

Z.F. Zhang et al., to be published in Phil. Mag.,2010

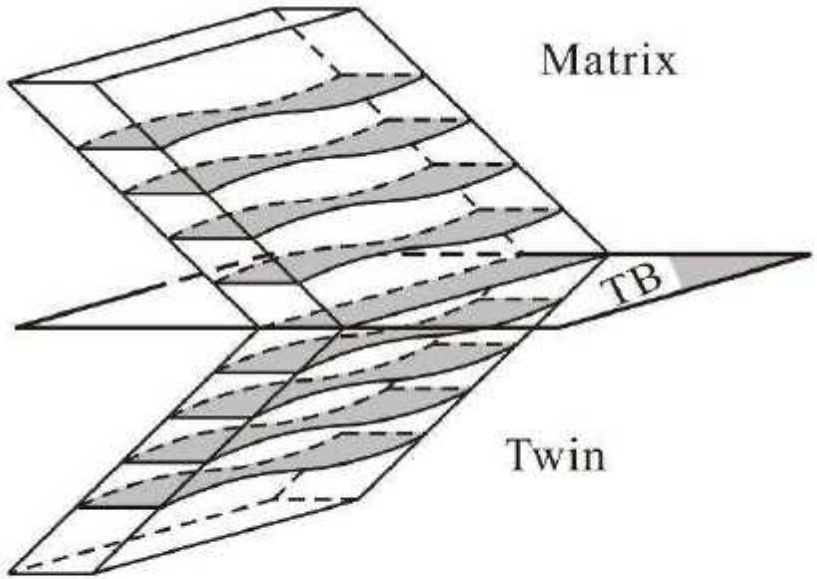

(c)

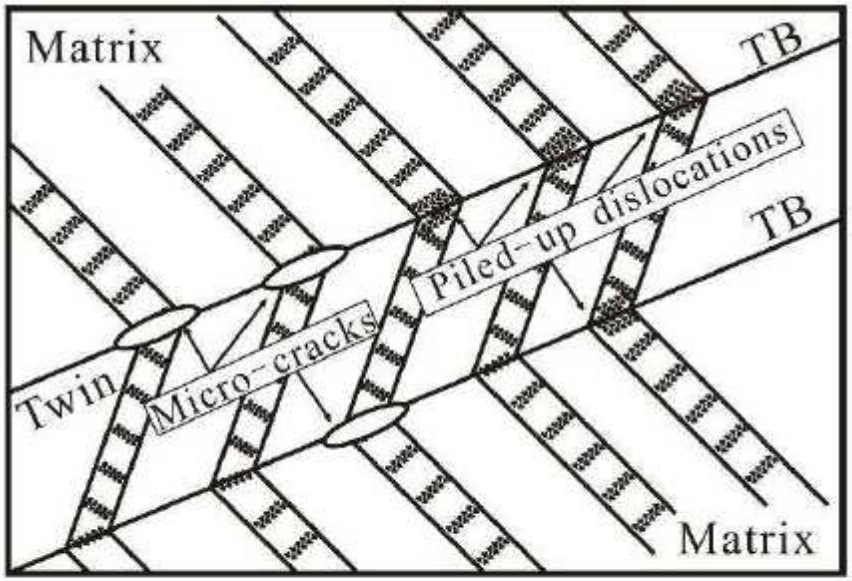

(d)

DEFORMATION ET RUPTURE DES ALLIAGES CFC A BASSE EFE

IMPORTANCE DU MACLAGE MECANIQUE

A.Pineau

Centre des Matériaux - Mines ParisTech

andre.pineau@ensmp.fr

Z.H.Zhang, Z.G. Wang, Acta Mater., vol.51, 2003, pp. 347-364

Cu BICRYSTALS

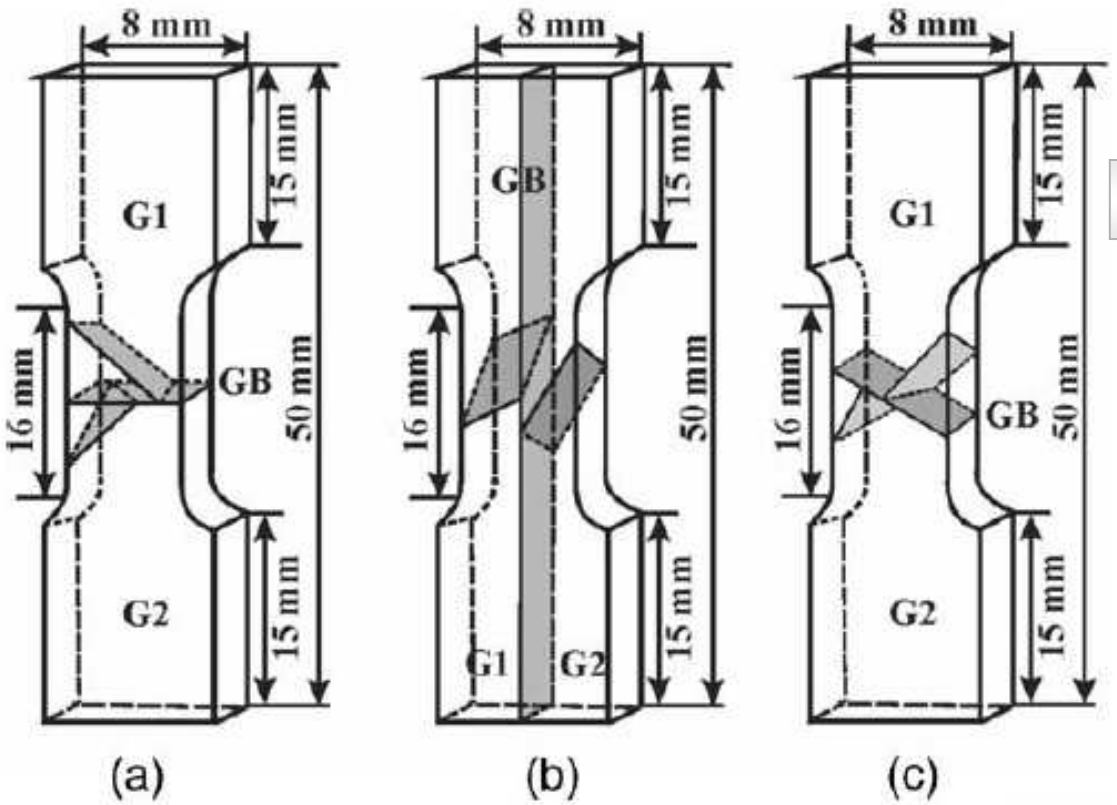

Fig. 2. Illustration of fatigue specimens and crystallographic relationships of the copper bicrystals with a large-angle GB perpendicular, parallel or tilting to the stress axis.

Z.H.Zhang, Z.G. Wang, Acta Mater., vol.51, 2003, pp. 347-364

Cu BICRYSTALS

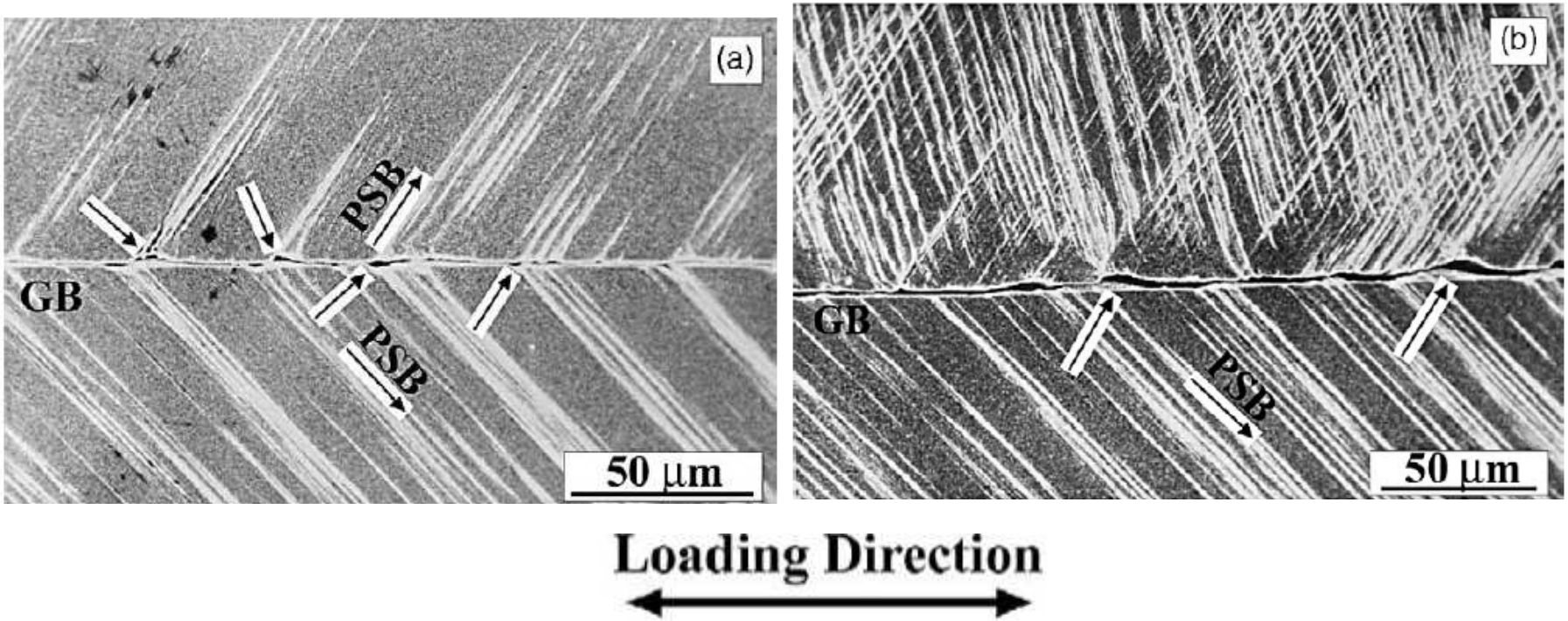

Fig. 8. Fatigue cracking along the GB parallel to the stress axis in the $[\bar{4}916]//[\bar{4}927]$ copper bicrystal deformed at low and high strain amplitudes for different cycles. (a) $\epsilon_{pl} = 5 \times 10^{-4}$, $N = 2 \times 10^5$; (b) $\epsilon_{pl} = 2 \times 10^{-3}$, $N = 2 \times 10^4$; (c) $\epsilon_{pl} = 2 \times 10^{-3}$, $N = 2 \times 10^5$.

B.Dyson, M.J.Rodgers, Mat. Science, 1974, vol.8, pp.261-266

NIMONIC 80A

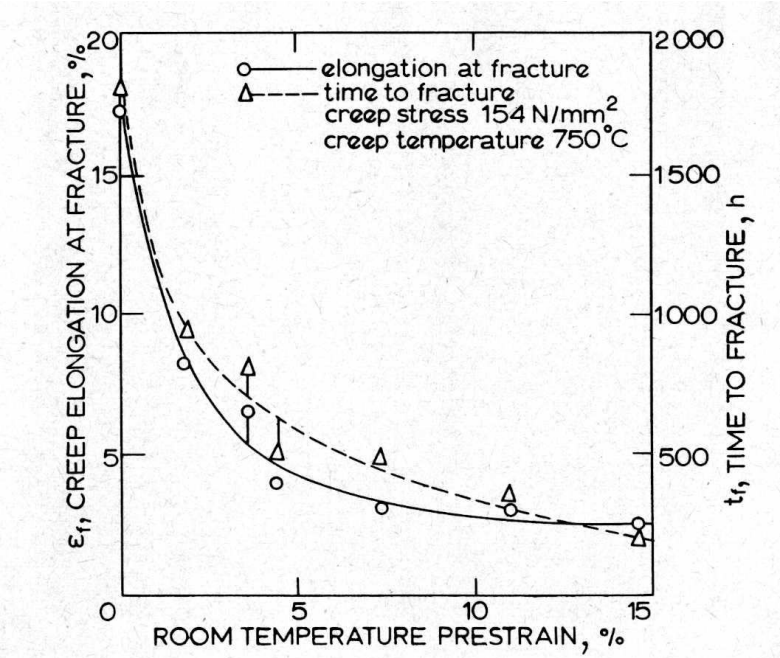

Fig. 1 Elongation and time to fracture of prestrained specimens crept at 154 N/mm² and 750° C.

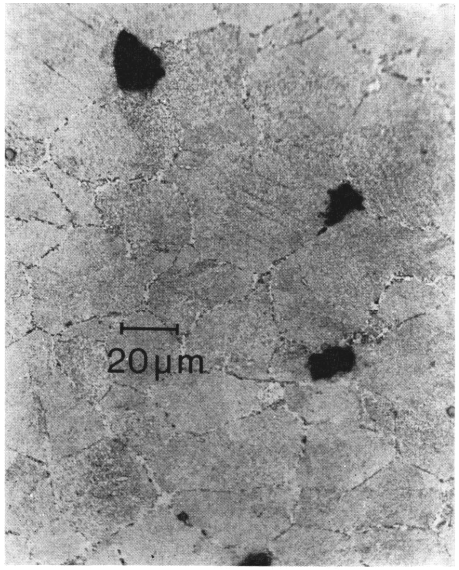

Fig. 4 Optical micrograph of an unprestrained specimen crept to fracture at 154 N/mm². Stress axis horizontal.

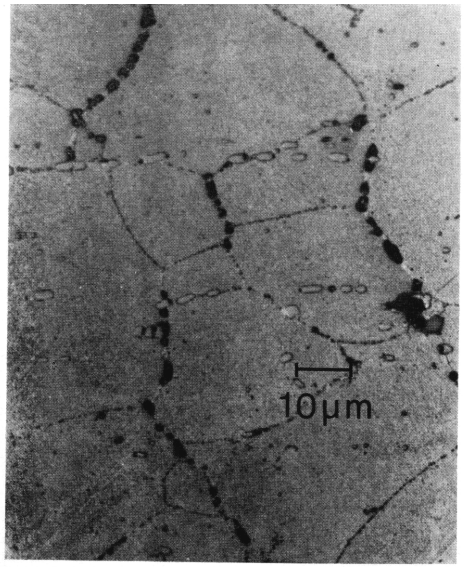

Fig. 6 Optical micrograph of a specimen prestrained by 14·8% and crept to fracture at 154 N/mm². Stress axis horizontal.

B.Dyson, M.J. Rodgers, Mat. Science, 1974, vol.8, pp.261-266

NIMONIC 80A

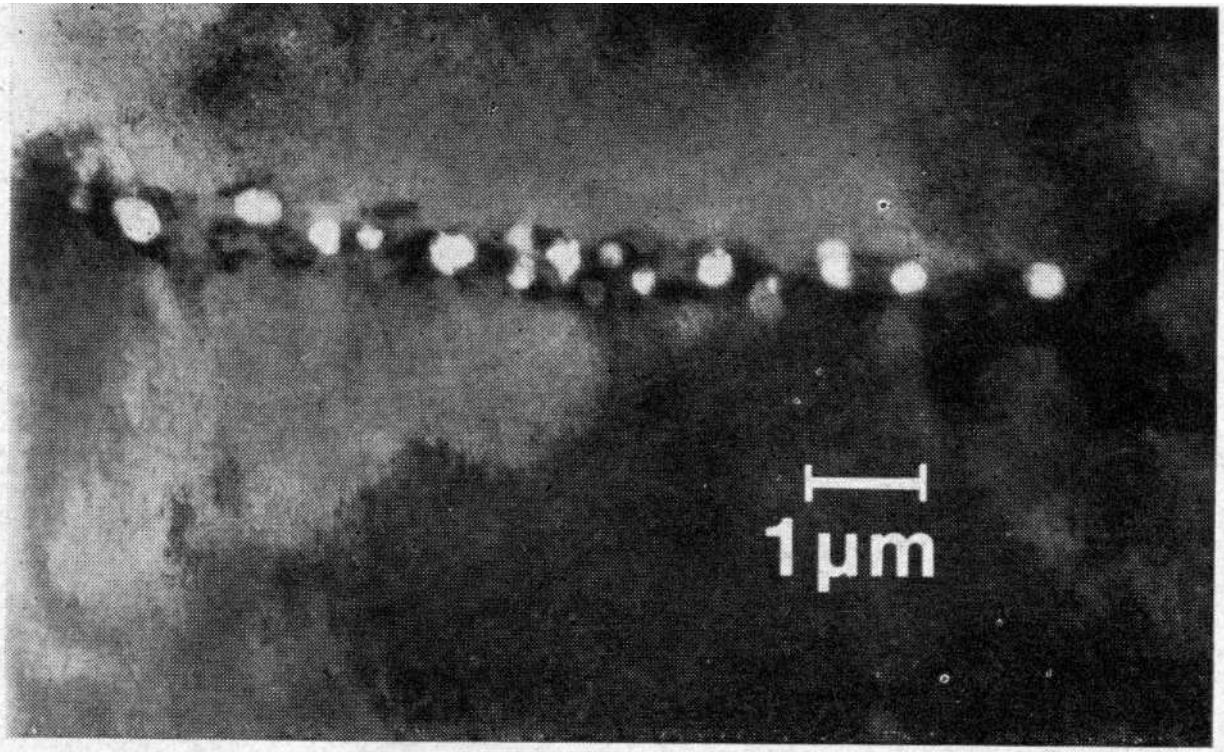

Fig. 11 1 MeV electron micrograph showing cavities on a grain boundary which is inclined to the electron beam. Specimen was prestrained 11% and annealed for 18 h at 750° C.

T.Saegusa, J. Wertman, Met.Trans, vol.11A, 1980, p1453

ASTROLOY

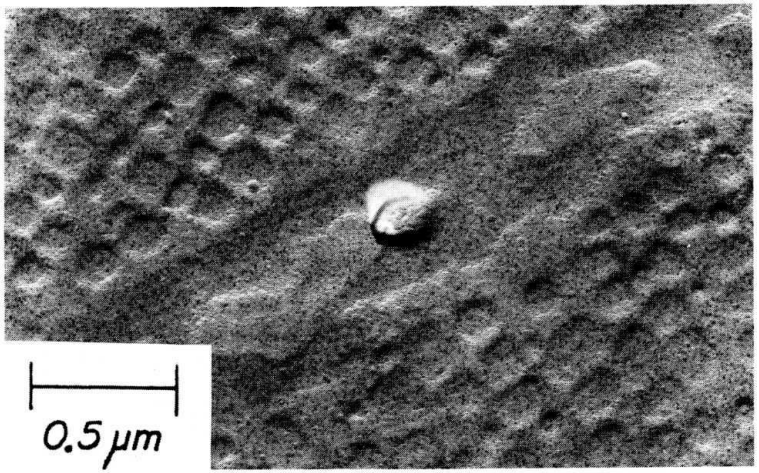

(a)

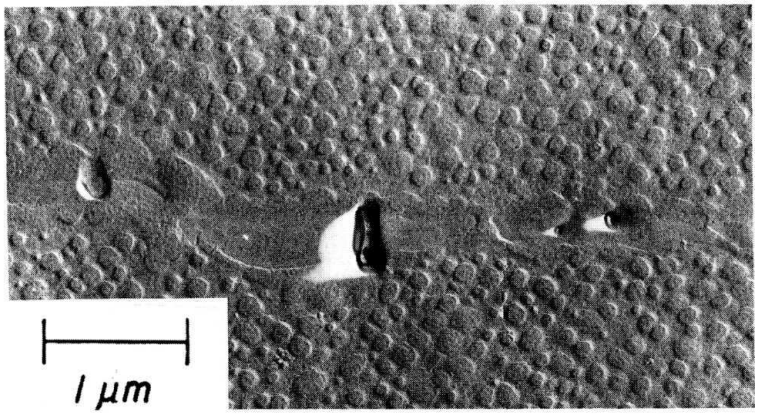

(b)

Fig. 7—Grain boundary voids in astroloy given H-3 heat treatment. Samples cold rolled through 15 pct RA, annealed at 810 °C for 2 h. Shadowing is perpendicular to the rolling direction in Fig. 7(*a*), parallel in Fig. 7(*b*).

Table III. Time to Failure of Samples of Prestrained and Nonprestrained Astroloy, Crept at 750 °C Under a Stress of 450 MPa*

Heat	Time to Failure, Hours	
	No Prestrain	Prestrained
1	286	11
2	89	8
3	>155	18
4	>110	20

* The prestrained samples had been cold rolled transverse to the stress axis through a 15 pct RA and annealed for 2 h at 810 °C.

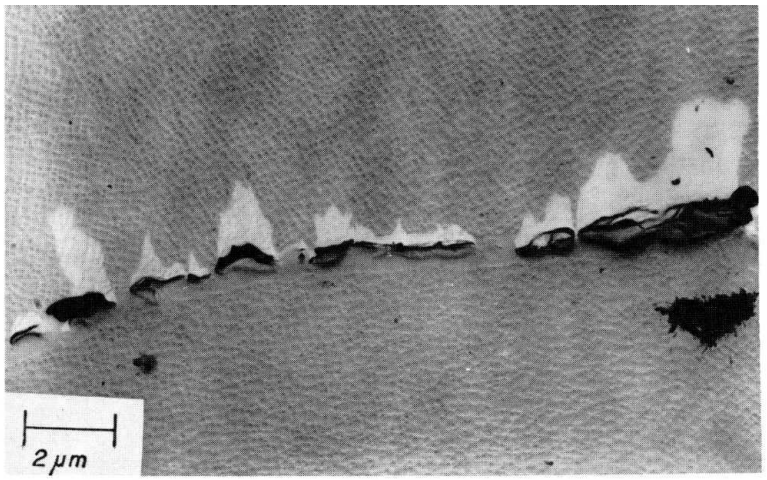

Fig. 13—Voids coalesced into secondary cracks in a sample of H-3 astroloy crept to failure at 750 °C under a stress of 450 MPa. Material not prestrained. Shadowing is parallel to the stress axis.

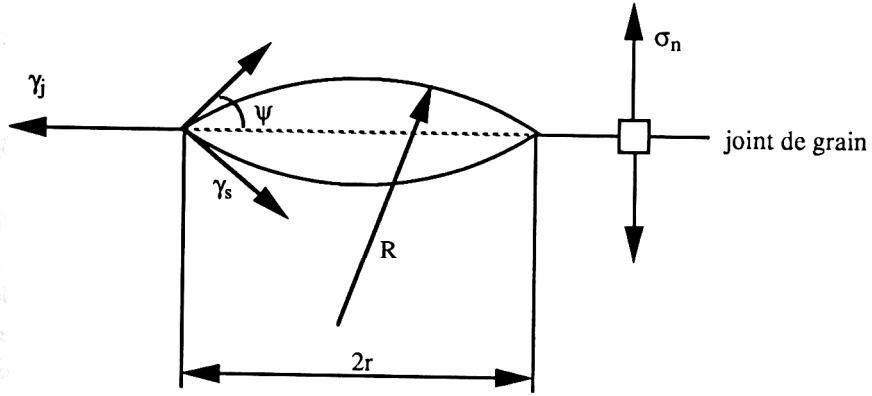

Figure 2.75. *Schéma d'une cavité lenticulaire sur un joint de grain d'énergie γ_j alors que l'énergie de surface vaut γ_S*

σ_n= 1000 MPa

Effect of Stress Concentration

$$\Delta G^* = \frac{8\pi}{3}\frac{\gamma_S^3}{\sigma_n^2}(1-\cos\psi)^2(2+\cos\psi)$$

$$R^* = \frac{2\gamma_S}{\sigma_n}$$

$$\dot{N} = \frac{2\pi R^* \sin\psi}{\Omega^{2/3}} \cdot \frac{\delta_j D_j}{\Omega^{2/3}} \cdot \exp\frac{\sigma_n \Omega}{kT} \exp\left(-\frac{\Delta G^*}{kT}\right)$$

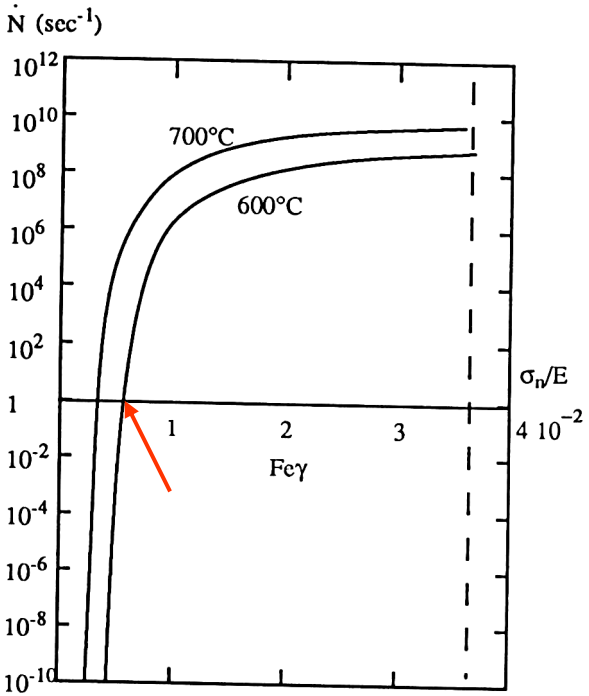

Figure 2.76. *Résultat de la théorie de la germination des cavités de fluage appliquée au fer. La vitesse de germination (sec^{-1}) est portée en fonction de la contrainte réduite appliquée sur le joint σ_n/E (où E est le module de Young)*

Devaux et al., Mat. Science & Eng. A, 486, 2008, pp. 117-122

INCO 718

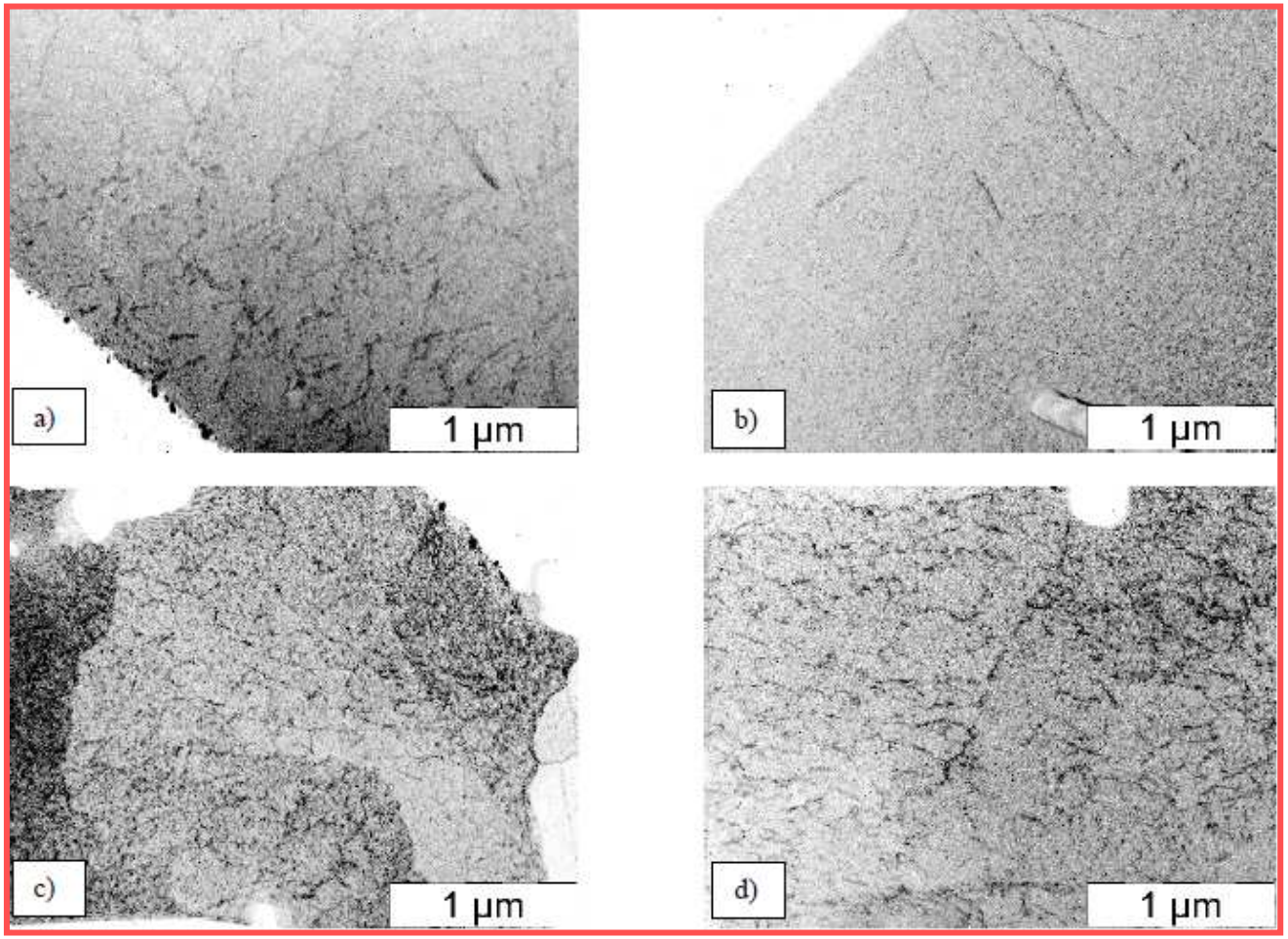

Dislocation densities (TEM) a) Zone 1; b) Zone 3; c) & d) Zone 4

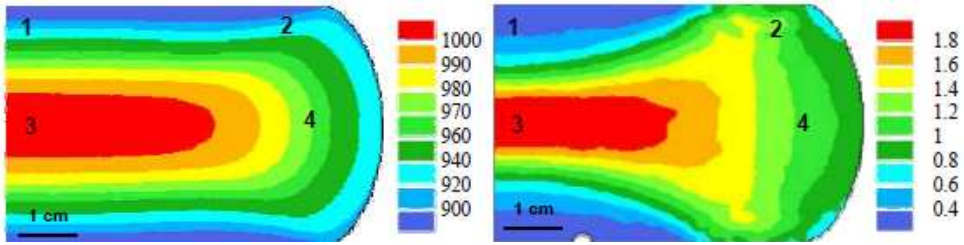

Devaux et al., Mat. Science & Eng. A, 486, 2008, pp. 117-122

INCO 718

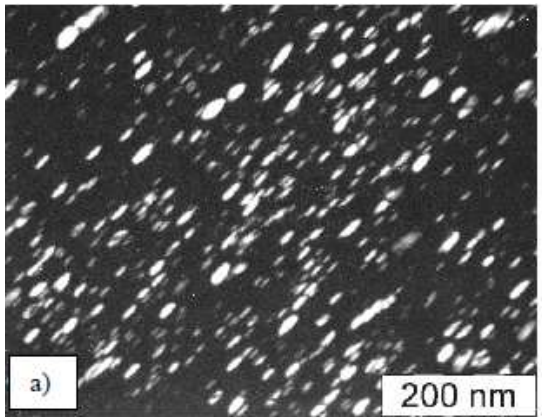

DA 718

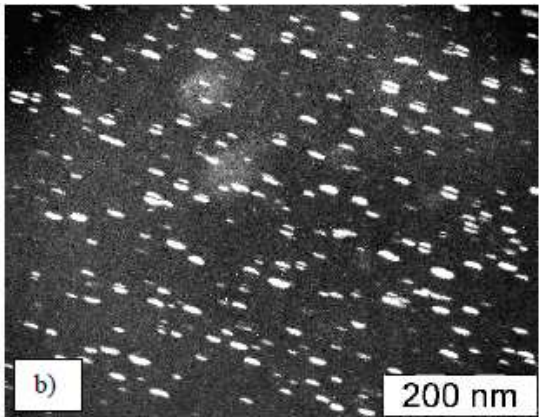

ST 718

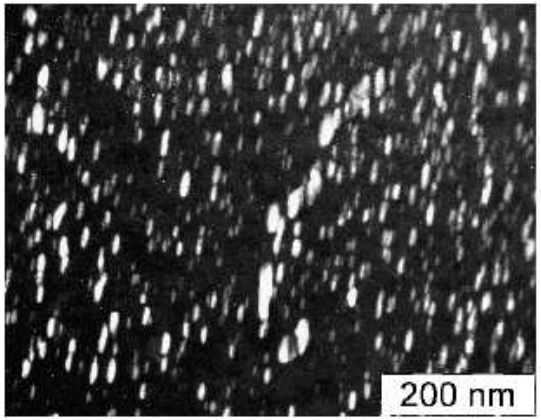

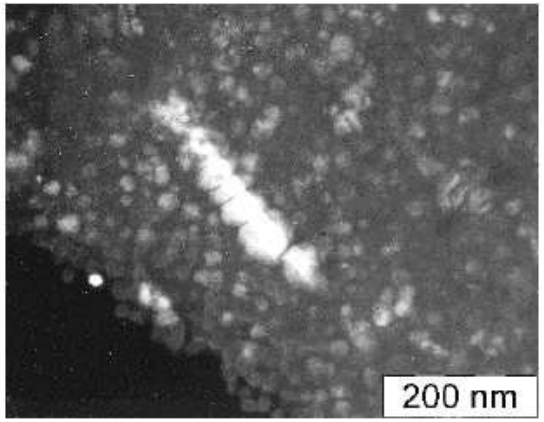

DA 718

CREEP CRACK GROWTH RATE IN ALLOY 718

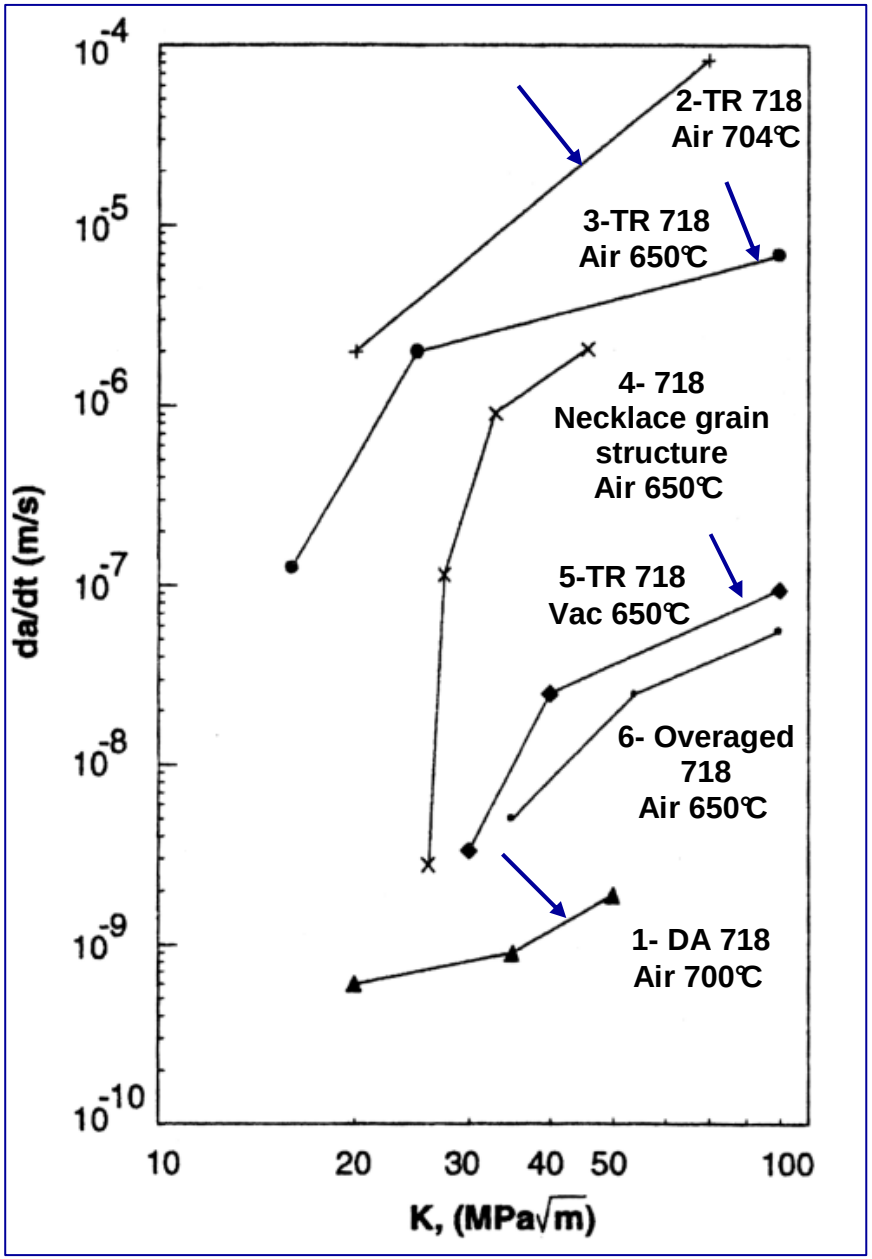

INFLUENCE OF MICROSTRUCTURE AND ENVIRONMENT

TR : AS QUENCHED (~950°C) + AGED (720°C - 8h + 620°C - 8h)

DA : DIRECT AGING (720°C - 8h + 620°C - 8h) after FORGING

DEFORMATION ET RUPTURE DES ALLIAGES CFC A BASSE EFE

IMPORTANCE DU MACLAGE MECANIQUE

A.Pineau

Centre des Matériaux - Mines ParisTech

andre.pineau@ensmp.fr

316 H C= 0.05 Wt %

Turski et al., Acta Mater., vol.56, 2008, pp 3598-3612

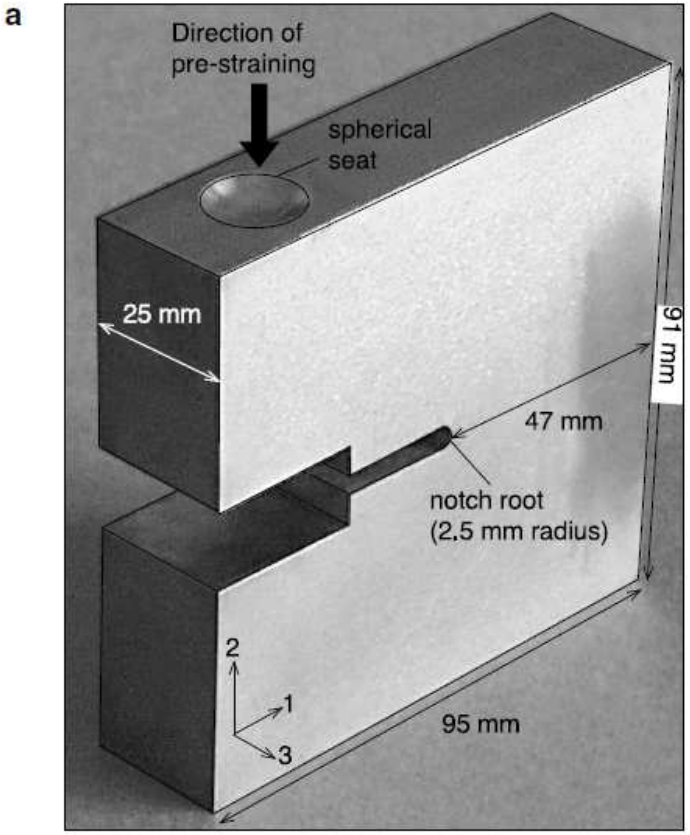

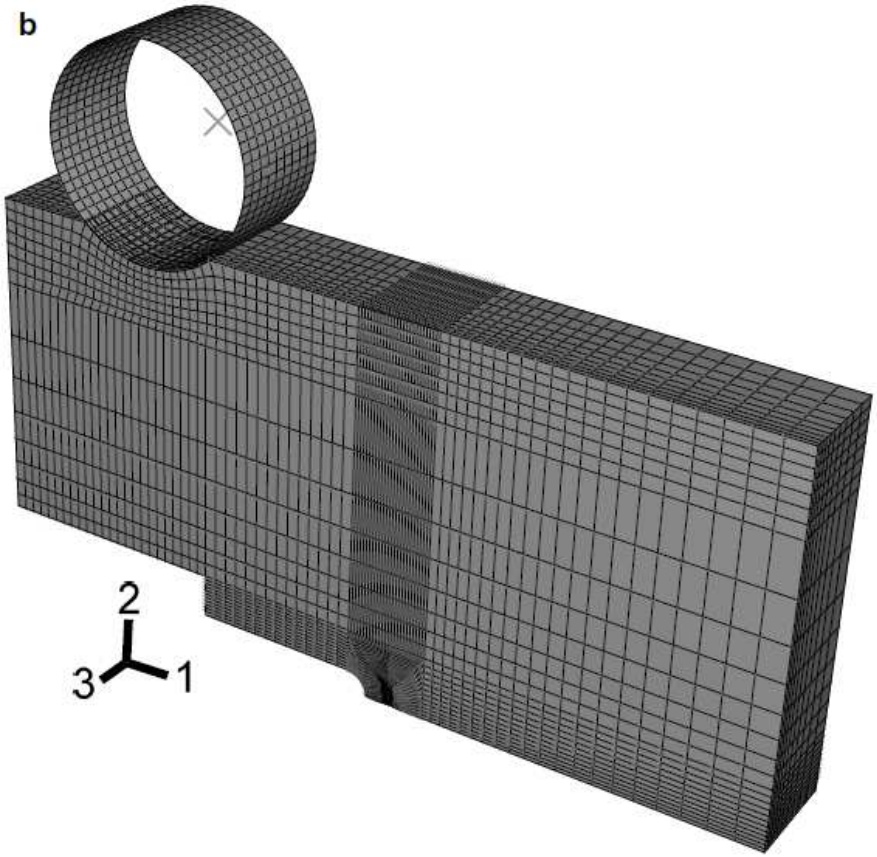

Déformation en Compression à 25℃
et Maintien en Température à 550℃ – 4500 heures

316 H C= 0.05 Wt %

Turski et al., Acta Mater., vol.56, 2008, pp 3598-3612

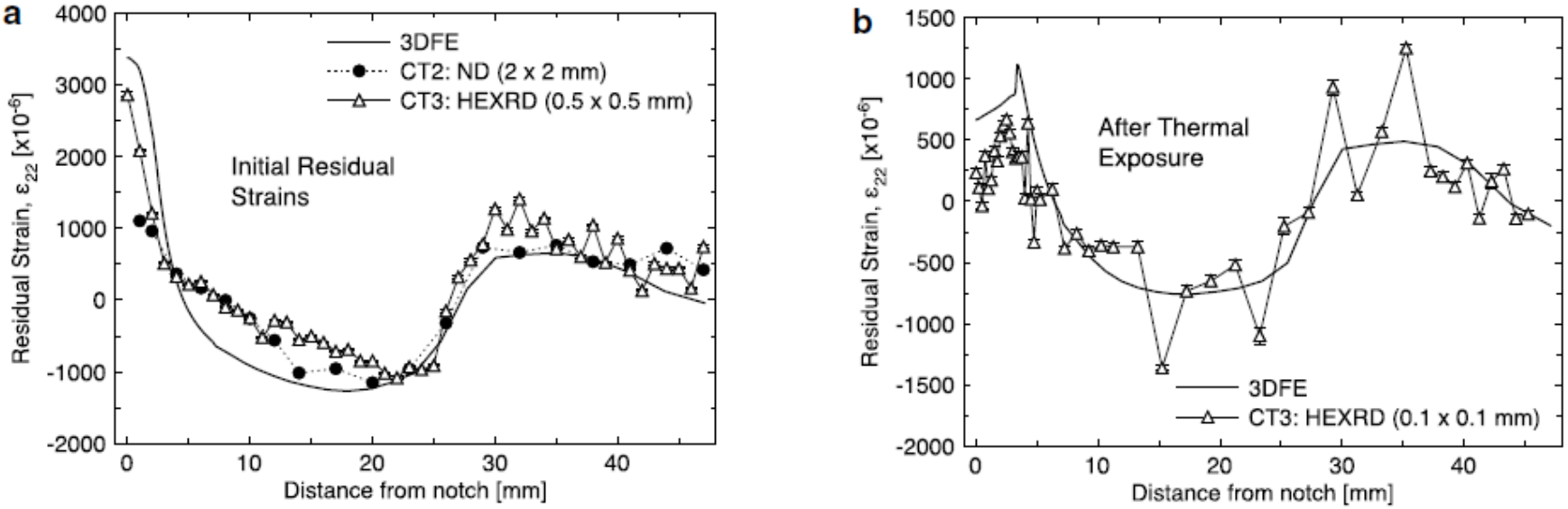

Fig. 4. Mid-thickness residual elastic strain measured by neutrons (diamonds), synchrotron X-rays (crosses) and predicted by 3-D FE for the notched CT specimens (CT3 and CT2) after pre-straining (a), and after subsequent thermal exposure for 4500 hours at 550 °C (b).

316 H C= 0.05 Wt % P

Turski et al., Acta Mater., vol.56, 2008, pp 3598-3612

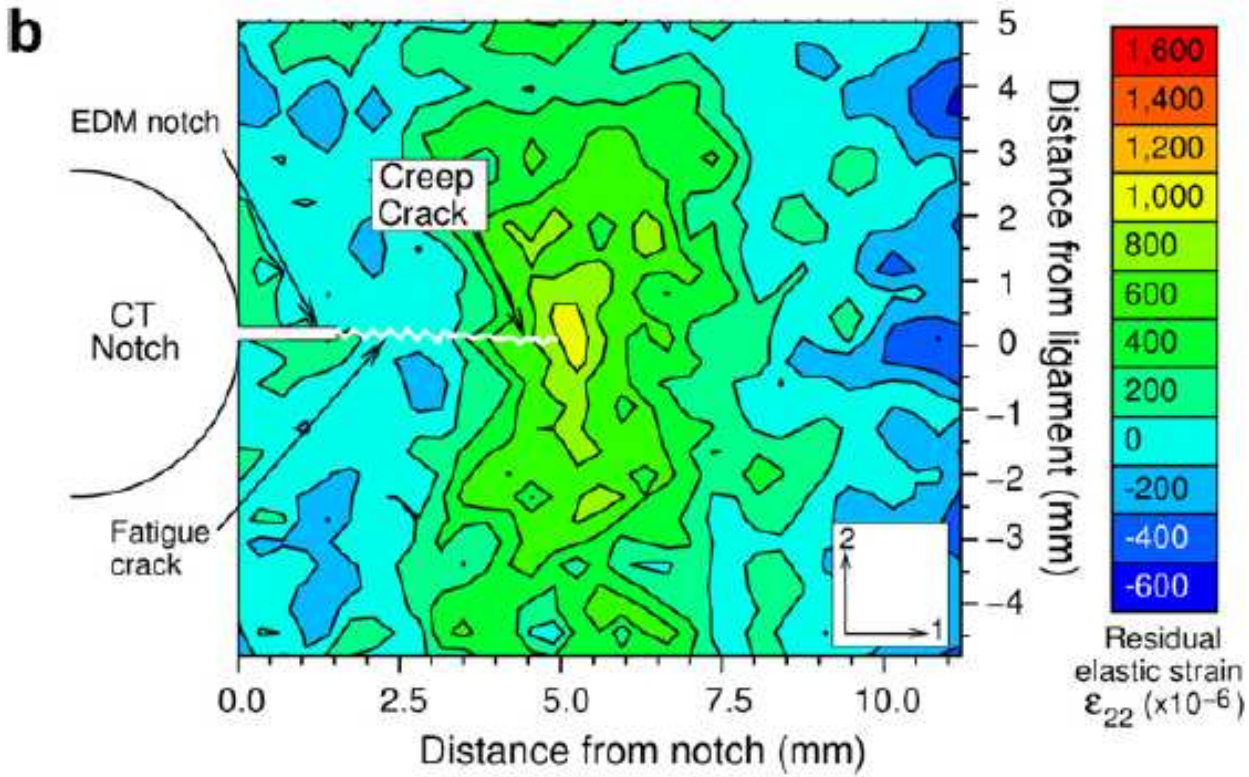

Fig. 5. Map of residual elastic strains measured around the crack tip region of CT1 (a) before (incident slits: 0.5 × 0.5 mm) and (b) after thermal exposure (incident slits: 0.35 × 0.35 mm) at 550 °C for 4500 hours. Notches and crack lengths have been drawn to scale.

Turski et al., Acta Mater., vol.56, 2008, pp 3598-3612

316 H C= 0.05 Wt % P

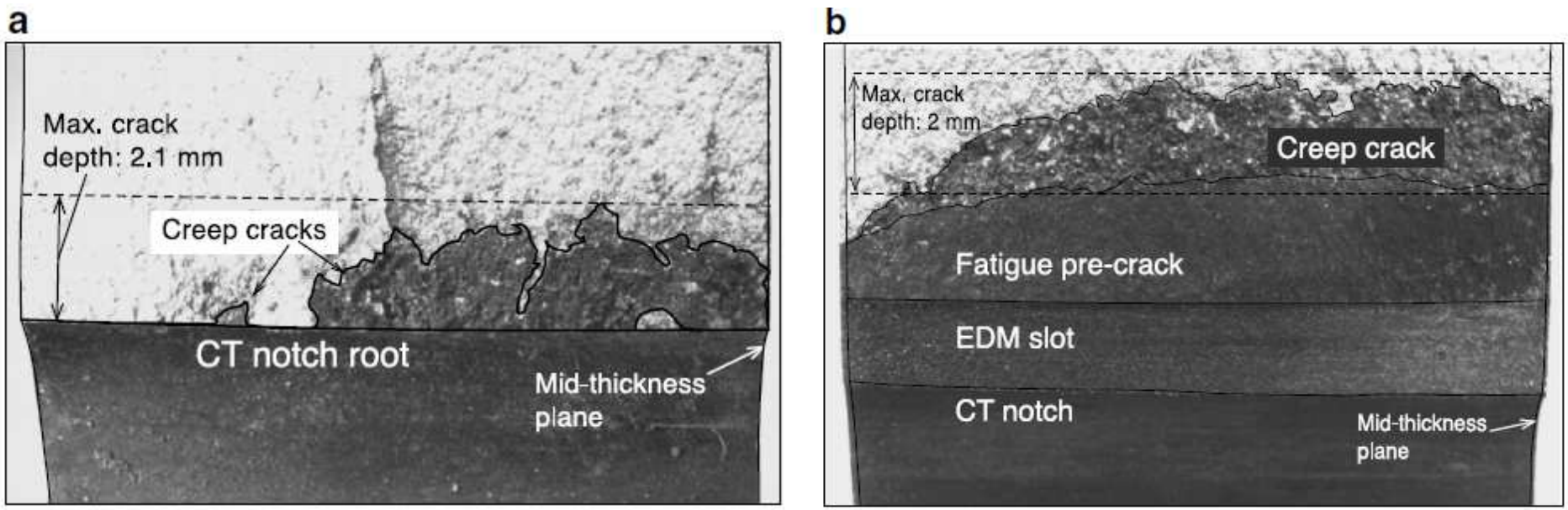

Fig. 7. Fracture surfaces for half of (a) the notched specimen CT3 (average creep crack length: 0.86 mm) and (b) the fatigue pre-cracked specimen CT1 (average creep crack length: 1.38 mm). For CT1, lines have been added to delineate the extents of the CT notch and EDM slot.

316 H C= 0.05 Wt % P

Turski et al., Acta Mater., vol.56, 2008, pp 3598-3612

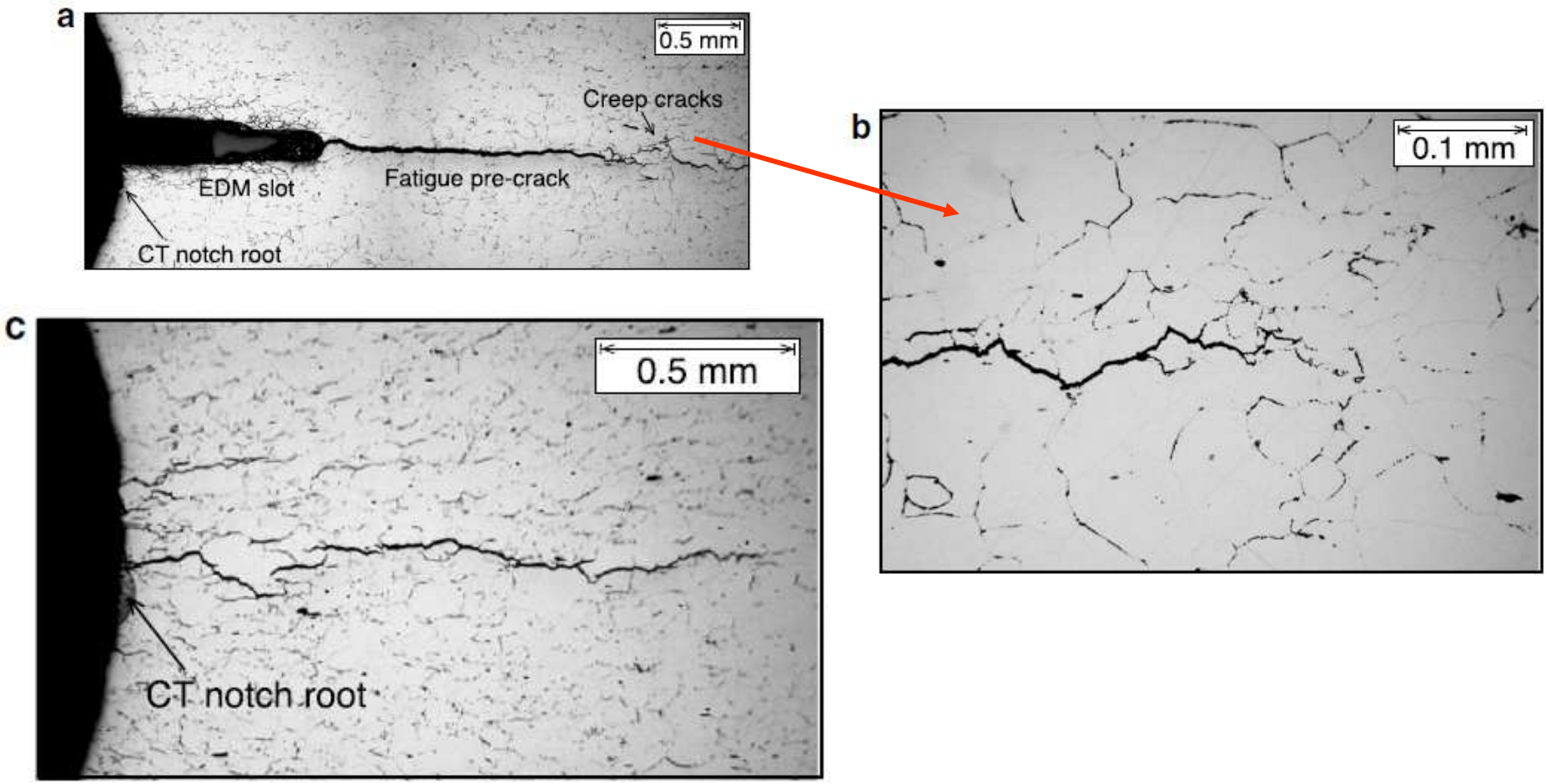

Fig. 8. Optical micrographs of the mid-thickness plane of (a) CT1, showing the notch root, EDM slot, fatigue pre-crack and creep crack; (b) CT1 showing close-up of the main creep crack tip – the formation of creep cavities can be seen forming along the grain boundaries and (c) CT3, showing a region of creep damage around the CT notch root.

DEFORMATION ET RUPTURE DES ALLIAGES CFC A BASSE EFE

IMPORTANCE DU MACLAGE MECANIQUE

A.Pineau

Centre des Matériaux - Mines ParisTech

andre.pineau@ensmp.fr

Table 1
Chemical composition (weight %) of the three studied AISI 316 stainless steels (bal. Fe).

Material	C	N	Cr	Ni	Mo	Mn	Si	Cu	S	P	Co	B
316L(N)	0.026	0.069	17.3	12.1	2.54	1.74	0.31	0.29	0.001	0.025	0.09	0.004
316H	0.05	0.033	17.1	12	2.32	1.48	0.52	–	0.01	0.02	0.05	0.003
316L	0.033	0.025	16.4	13.6	2.12	1.55	0.44	<0.07	0.024	0.022	0.18	0.001

Tableau 1. Compositions chimiques en pourcentages massiques des aciers étudiés.

Matériau	N	C	Mn	Cr	Si	Ni	Mo	S	Ti	P	Co	Cu	Nb	B
AISI 321	0,014	0,06	1,63	18,0	0,49	10,2	0,23	0,012	0,56	0,024			<0,05	0,0018
AISI 304H	0,034	0,059	1,23	18,4	0,68	11,8	0,33	0,03	<0,02	0,028		0,12	<0,05	<0,0005
AISI 316L(N)	0,068	0,029	1,73	17,3	0,31	12,1	2,53	0,001		0,023	0,089	0,29		0,0003

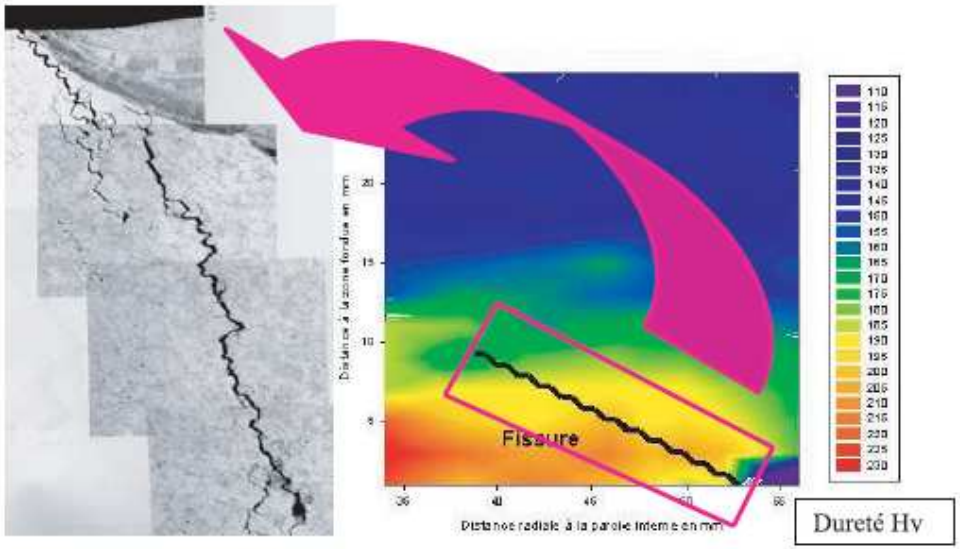

Fig. 5. Cas d'une fissuration intergranulaire observée sur un composant en acier AISI AISI 304H et cartographie de dureté Hv de la zone affectée.

Q. Auzoux et al. , JNM , vol.400,(2010), pp.127-137

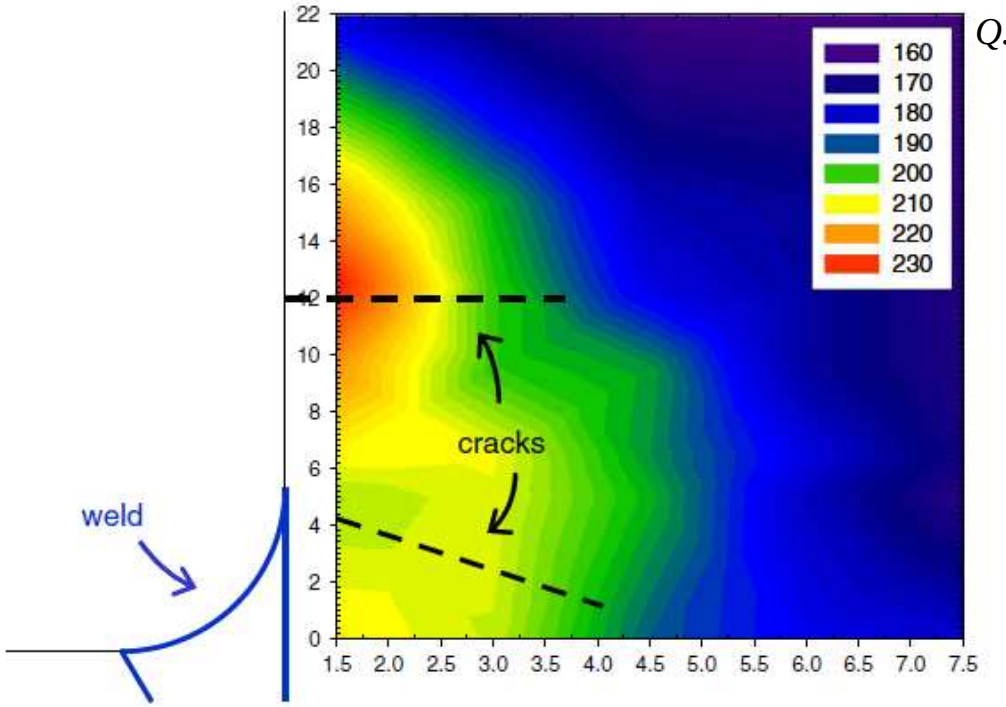

Vickers hardness map (30 kg) around reheat cracks near an as-received weld of 316H steel, indicated dimensions are in millimetres.

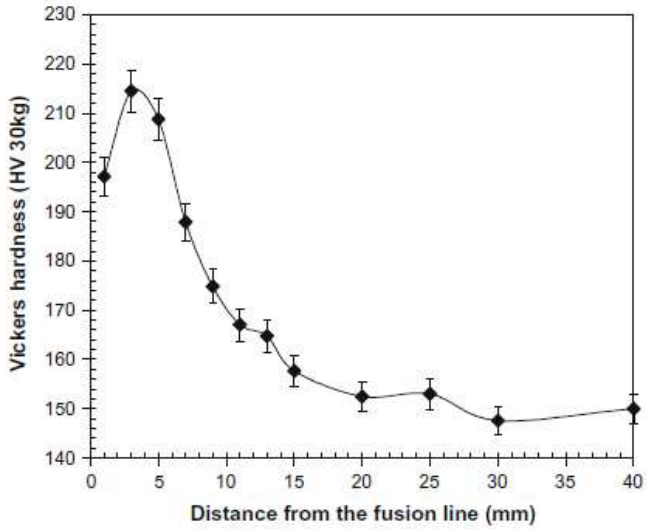

Fig. 2. Vickers hardness under 30 kg near an uncracked as-received weld in 316H.

Q. Auzoux et al. , JNM , vol.400,(2010), pp.127-137

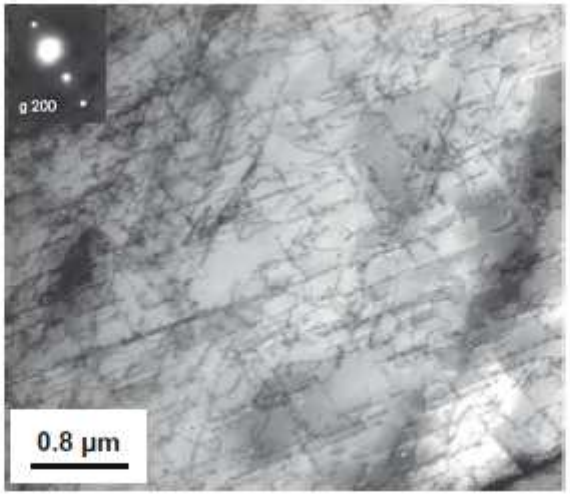

Fig. 4. Dislocation microstructure of as-received 316H base metal (bright-field TEM imaging).

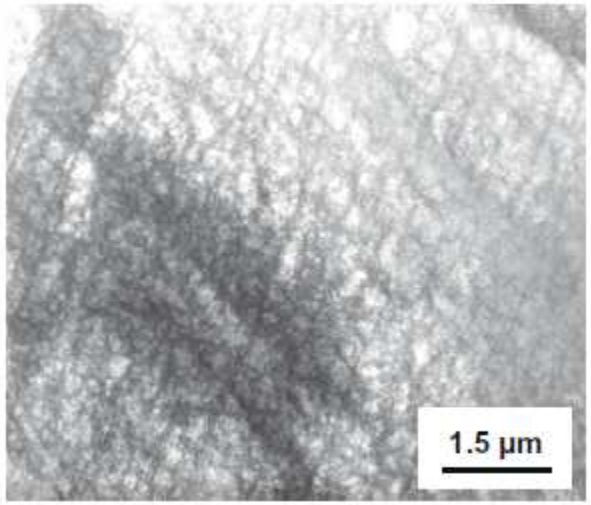

Fig. 3. Dislocation microstructure of as-received weld-affected zone of 316H, 0.2 mm away from the fusion line (bright-field TEM imaging).

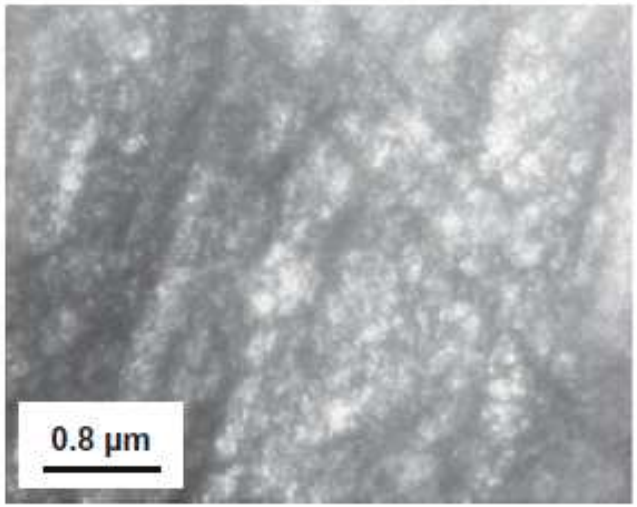

Fig. 8. Dislocation microstructure of pre-strained 316H (bright-field TEM imaging).

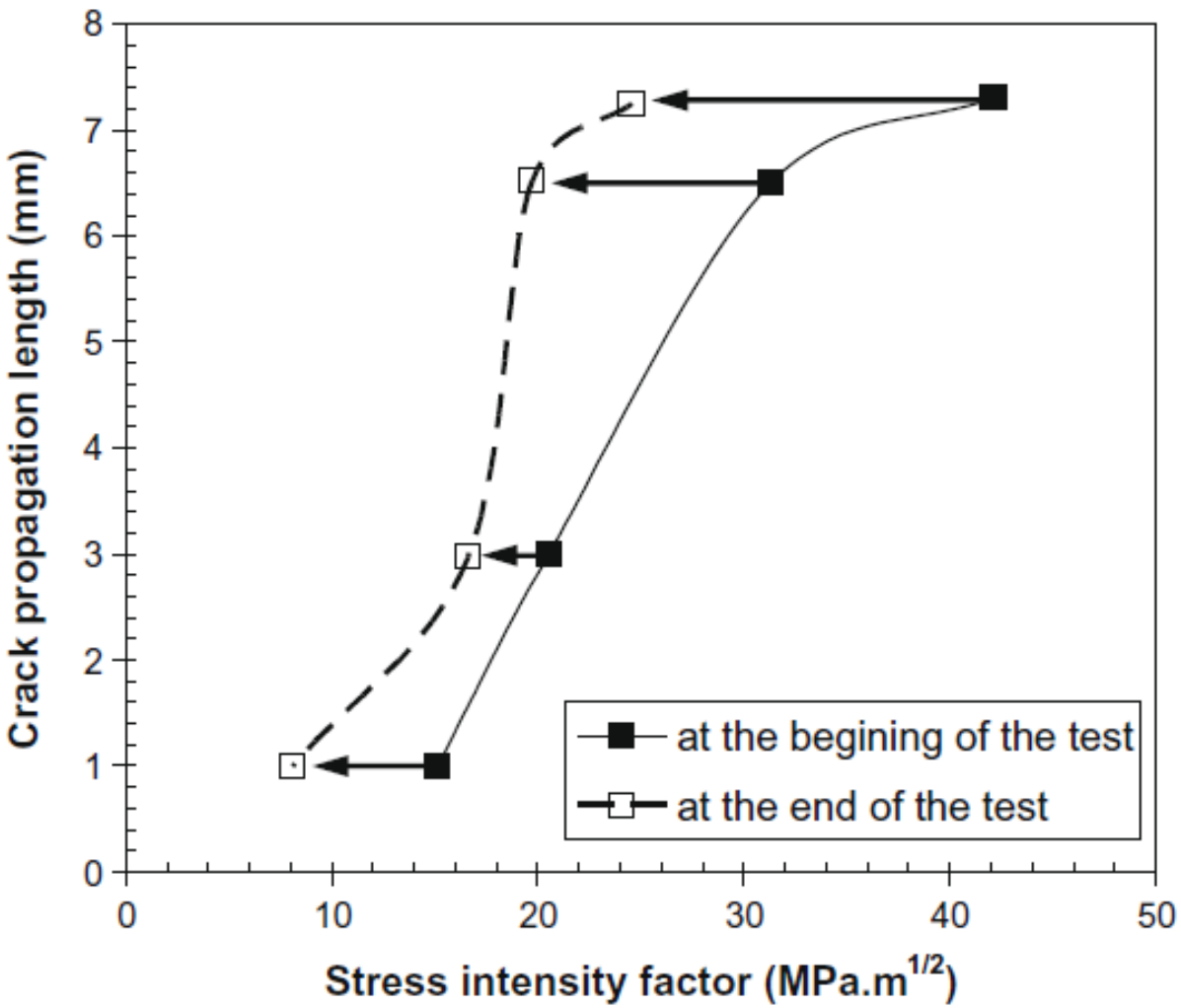

Fig. 10. Crack propagation length during relaxation for 600 h at 600 °C on pre-strained 316H pre-cracked CT specimens versus the stress intensity factor, which is calculated both at the beginning and at the end of the test.

Table 5
Results of relaxation tests at 600 °C on pre-cracked CT specimens.

Material	State	a_0/W	Initial stress intensity factor (MPa $\sqrt{m}$)	Final stress intensity factor (MPa $\sqrt{m}$)	Opening (μm)	Test duration (h)	Crack propagation length (mm)
316L(N)	Annealed	0.499	25	15	248	1004	0.0
316L(N)	Annealed	0.501	31	18	578	1006	0.0
316L(N)	Pre-strained	0.494	41	22	214	619	2.4
316L(N)	Pre-strained	0.493	30	18	136	608	1.5
316L(N)	Pre-strained then aged 2 h at 700 °C	0.503	42	30	231	652	1.8
316H	Annealed	0.503	31	23	803	652	0.5
316H	Pre-strained	0.494	41	27	200	571	7.3
316H	Pre-strained	0.490	30	21	114	577	6.5
316H	Pre-strained	0.496	20	18	116	598	3.0
316H	Pre-strained	0.491	15	9	68	597	1.0
316L	Pre-strained	0.500	42	28	291	206	9.8
316L	Pre-strained then aged 2 h at 700 °C	0.498	42	35	201	205	2.8

Q. Auzoux et al. , JNM , vol.400,(2010), pp.127-137

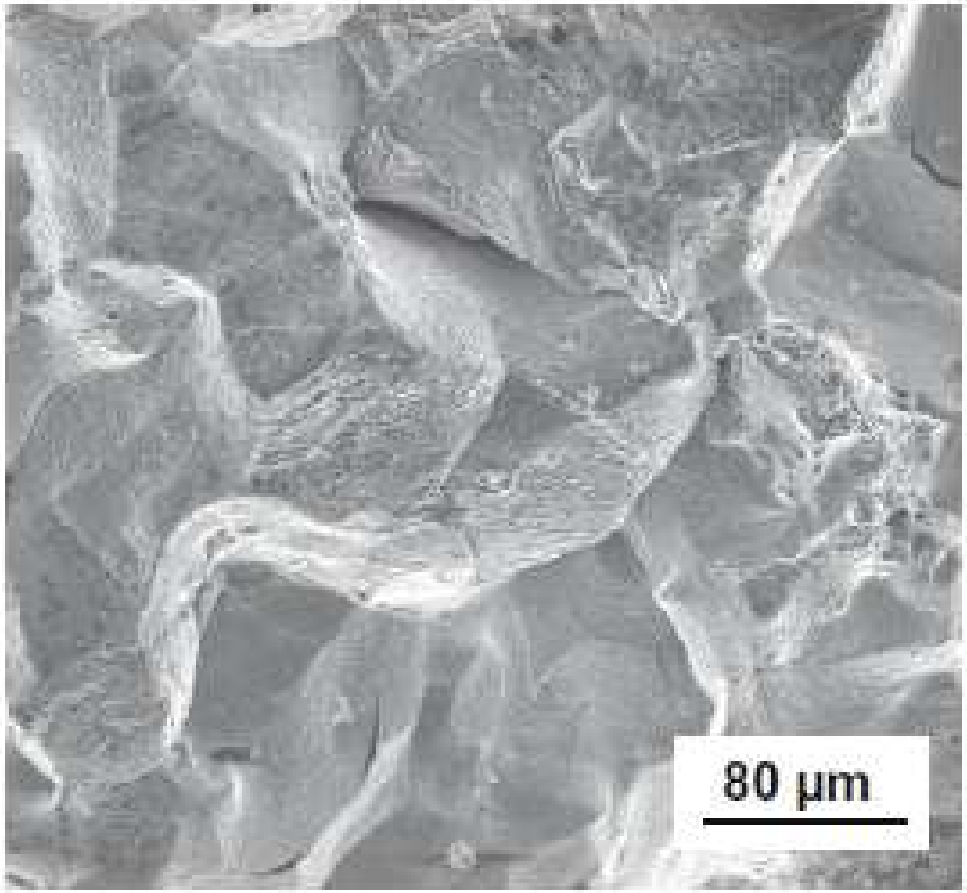

(a) Pre-strained 316H

Fracture surface of prestrained 316 H Steel tested at 600°C

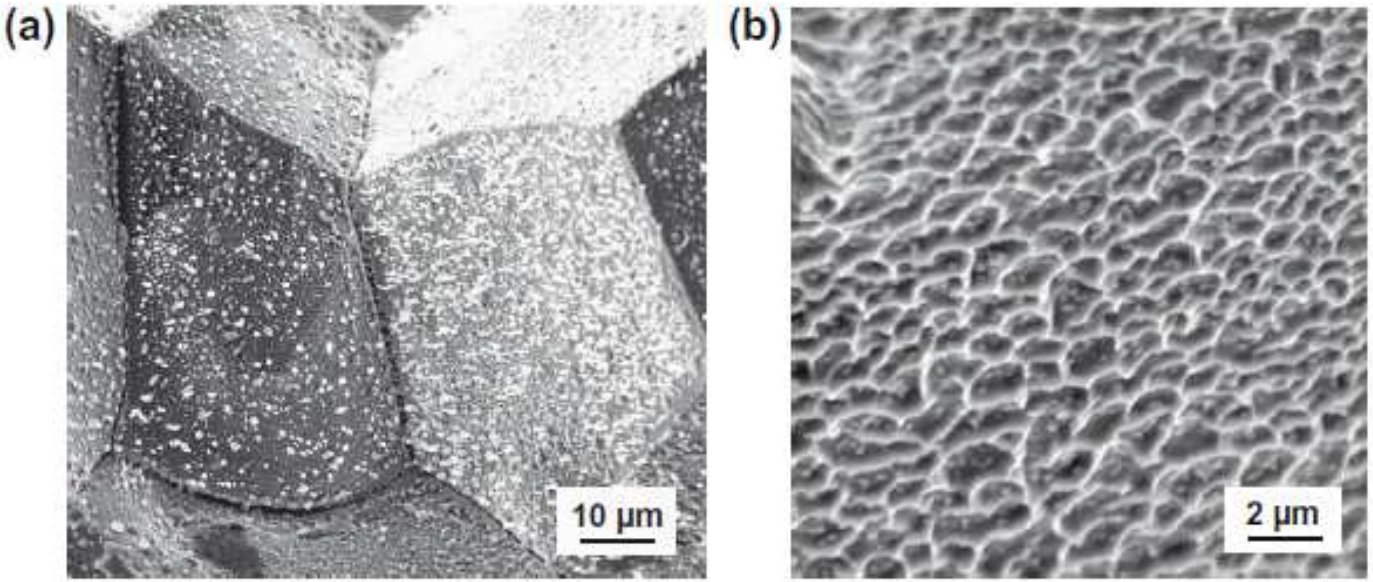

Fig. 13. Fracture surfaces after relaxation at 600 °C of pre-strained 316H pre-cracked CT specimens (secondary electron SEM images), (a) relatively low magnification image of intergranular facets, (b) higher magnification image showing micro-dimples on an intergranular facet.

Q. Auzoux et al. , JNM , vol.400,(2010), pp.127-137

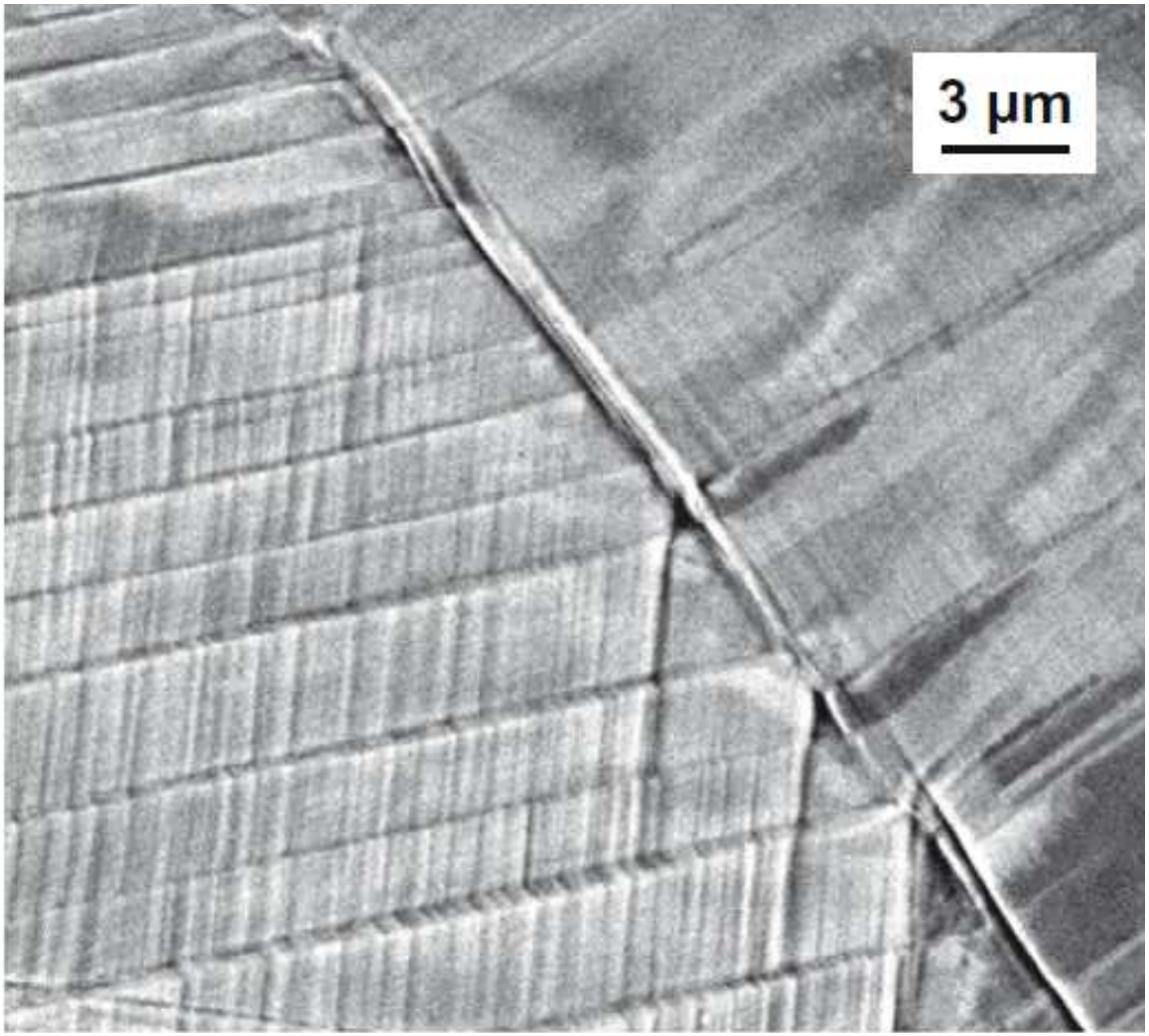

DEFORMATION ET RUPTURE DES ALLIAGES CFC A BASSE EFE

IMPORTANCE DU MACLAGE MECANIQUE

A.Pineau

Centre des Matériaux - Mines ParisTech

andre.pineau@ensmp.fr

CONCLUSIONS

- Les Problèmes de Mode!
- Many Researches on Mechanical Twinning in FCC Metals are needed:
  - Nucleation still poorly understood
  - Relatively Strong Strain Rate Sensitivity of Low SFE FCC Metals
  - More Detailed Observations of Slip/Twin and Twin/Twin Intersections
  - Twin Boundaries Weak or Strong?

Monotonous – Fatigue- Creep Loadings

MERCI POUR VOTRE ATTENTION

Bureau B 110

Tel : 06 83 10 57 76

andre.pineau@ensmp.fr